THE FRICTION MEASURING MACHINE: AN ENERGY-BASED APPROACH TO FRICTION CHARACTERIZATION

by

Christian Theodore Lomascolo

A thesis submitted to the faculty of
The University of North Carolina at Charlotte
in partial fulfillment of the requirements
for the degree of Masters of Science in
Mechanical Engineering

Charlotte

2017

Approved by:

_____
Dr. Tony Schmitz

_____
Dr. John Ziegert

_____
Dr. Stuart Smith

ABSTRACT

CHRISTIAN THEODORE LOMASCOLO. The Friction Machine: An Energy-Based Approach to Friction Characterization (Under the direction of DR. TONY L. SCHMITZ)

Friction has been studied and analyzed through the years. The need for precise friction measurement has become increasingly important as the need for precision positioning mechanism has increased. This precise control of mechanical systems requires the knowledge of specific parameters in the system. A subset of these parameters is the friction model. Traditionally, friction models are parameterized using steady-state force measurement during sliding contact. In this thesis, a new displacement-based friction measurement machine is designed and constructed, where linear motion is prescribed using a parallelogram leaf-type flexure. The flexure has a natural frequency of 2.24 Hz, a stiffness of approximately 1955 N/m (the average of the two different tests), and a viscous damping ratio of 0.00085. The parasitic motion at a displacement amplitude of 10 mm is less than 0.1 μm and the uncertainty of the relative position of the two samples due to structural deflection is 1 μm.

ACKNOWLEDGMENTS

I would like to acknowledge my advisor, Dr. Tony Schmitz, for his continued guidance throughout the duration of this experience. I would also like to thank him for the opportunity to be a part of this research. This experience has helped me to grow both personally and as an engineer. I would also like to thank Dr. John Ziegert, Dr. John Brien, Dr. Stuart Smith, and Dr. Jimmie Miller for their assistance throughout this effort.

I would like to thank Dr. Chris Tyler for teaching me how to use various equipment that was crucial to the development and validation of this research. I would also like to thank my family and friends for supporting and encouraging me throughout this experience.

TABLE OF CONTENTS

LIST OF TABLES

LIST OF FIGURES

LIST OF ABBREVIATIONS

DMI	Displacement Measuring Interferometer
FMM	Friction Measuring Machine
PTFE	Polytetrafluoroethylene

CHAPTER 1: INTRODUCTION

Friction is inherence in physical contacts, whether moving or static, and varies with environmental and boundary conditions. Force-based methods exist to determine friction coefficients for a variety of friction models. These methods measure the surface normal and friction forces using load cells during translational or rotational relative motion between a pair of samples. Because friction measurement includes contact, wear occurs with a corresponding breakdown of the softer sample. This causes the friction coefficient to vary with the sliding distance. The use of force transducers to determine the friction model coefficients leads to relatively high uncertainty (parts in 10^2). As an alternative, this research proposes a displacement-based approach to identifying friction coefficients. Because displacement measuring interferometry (DMI) offers lower uncertainty than force measurement, in general, the end goal is to reduce friction measurement uncertainty by this displacement-based strategy. In this thesis, a friction measuring machine (FMM) is designed to implement the new approach.

For the new FMM, a flexure-based design with a gravity-based normal load is implemented to reduce measurement uncertainties. This is critical when measuring very low coefficients of friction, such as the friction in air bearings or rolling contacts. The motion of the flexure during free vibration due to an initial displacement is measured for two cases: first, with no friction contact; and second, with friction contact. The difference in the energy loss in the system due to friction.

CHAPTER 2: LITERATURE REVIEW

Friction measurement can be described as the ratio of sliding force (or force to initiate sliding) to the normal force between the contacting surface. Parameterizing the friction model for two samples in contact requires precise measurement techniques. In this thesis, displacement measurement during free vibration of a flexure mechanism subjected to some initial conditions is employed to define the friction model.

Over the years many models have been used to characterized the phenomena of friction. These models include the Dahl model [1], Bristle model [2], Reset Integrator model [2], lubrication models, LuGre model [3], and various others [4]. In the bristle model, for example, microscopic contact points are described by bonds between flexible bristles [4]. The strain in the bristles during relative motion acts as a spring and therefore produces friction force. New models to describe friction behavior are being developed constantly and need to be validated. The friction measurement machine proposed in this research introduces a method for verifying these models.

Friction compensation through control loops is a direct way to overcome the undesirable results due to friction [4]. To compensate for friction in the control strategy, precision characterization of the behavior of friction is required as an input. In [5], traditional tribology experiments were conducted using a pin-on-disk approach, where a force transducer measures the normal force being applied to the pin and the resulting friction force generated at the interface between the two samples. The lack of precision in force transducers and their alignment with the applied force direction leads to measurement

uncertainty. The use of alternate measurement techniques, such as laser interferometry, can reduce the measurement uncertainty.

A displacement measuring interferometer (DMI) offers a high resolution/range displacement transducer. For low uncertainty measurement, environmental compensation must be applied. In [6], corrections for Abbe, cosine, deadpath, and environmental errors are described and the associated uncertainty is evaluated.

Proper flexure design is key in the development of the FMM. In his 2000 publication, Smith [7] describes flexure limits and performance of flexure elements. Flexures enable smooth uninterrupted motion without the use of joints or sliding components. In [8], Schmitz and Smith describe methods for characterizing single degree-of-freedom free vibration systems as lumped parameter spring-mass-dampers.

CHAPTER 3: BASIS OF DESIGN

The basis of the FMM design is a single degree-of-freedom flexure. A single degree-of-freedom flexure is stiff in five of the six directions and flexible in one axis. The fundamental goal of the FMM is to associate displacement with friction. Since the results from the tests performed with the FMM machine are solely dependent on a single DMI the machine must be able to isolate other means of energy dissipation that are not related to the energy loss recorded by the DMI. Besides the flexure, a rigid method of holding a sample while applying a consistent measurable force is required. An air bushing is considered to be near frictionless at very low speeds and would not create any unwanted forces on the shaft. The major design considerations are discussed in the following paragraphs.

A symmetric flexure design was used to best approximate a linear stiffness over the active range of the flexure. Symmetry was also utilized in the design of the moving platform. The moving platform was placed both vertically and horizontally in the center of the flexure. Since the frictional force is being applied to the moving platform, it is beneficial to measure along the same axis as the force is being applied.

Reducing the Abbe offset to near zero, assuming the force is being applied in the same axis as the measuring device, enables the errors caused by deformation of the active object to be minimized. The symmetric design helped to reduce errors caused by uniform thermal growth that could otherwise cause the assembly to rotate and deform.

The machine was intentionally overdesigned to assure that key areas of the design are very stiff, which allows for certain assumptions to be made when performing design calculations. The base that houses the air bearings and accompanying shaft is a solid slab of aluminum. This base is responsible for rigidly holding the sample, which is necessary since this is assumed in the model.

As noted, the major design considerations that motivated the FMM are stiffness, Abbe offset, and, most importantly, symmetry. Using these basic concepts enabled an iterative process of fine tuning design parameters, including flexure length, stiffness, and geometry, as well as air bushing location and size. For reference throughout the subsequent chapters, Figure 1 displays the proposed flexure design.

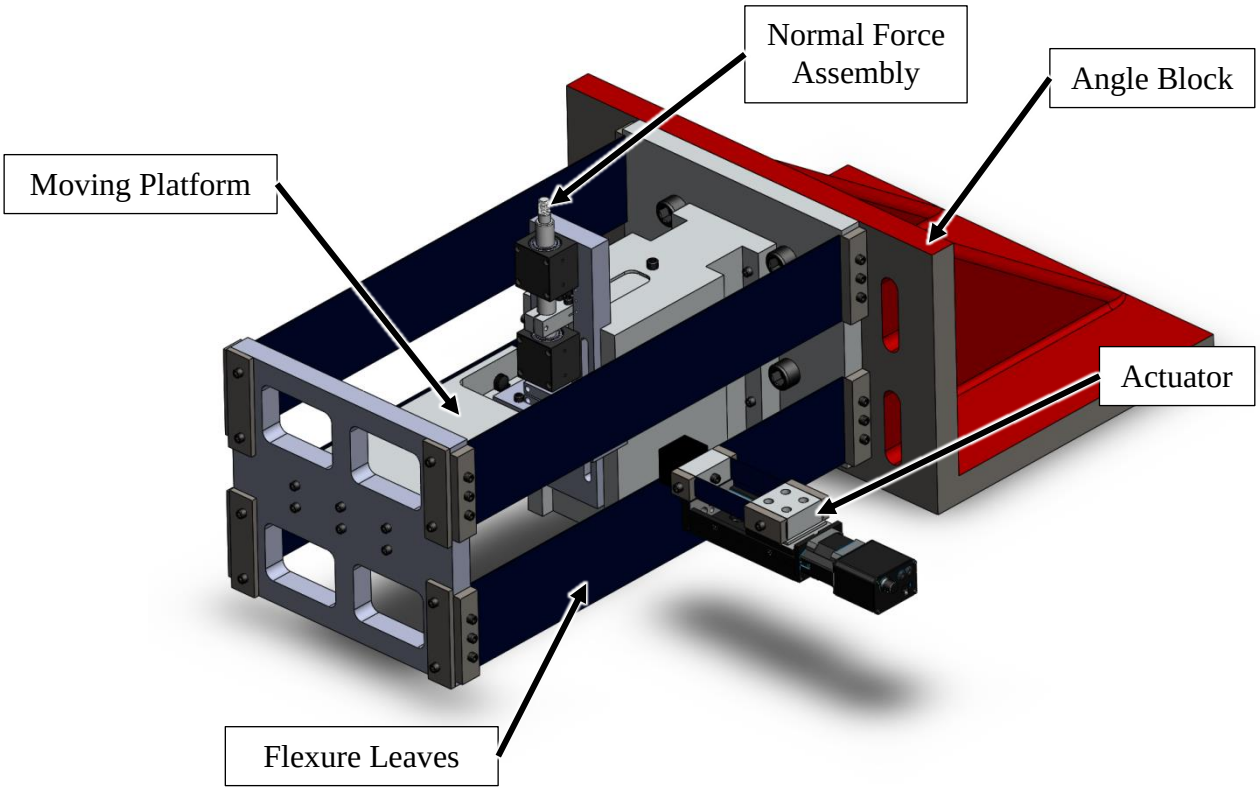

Figure 1: Flexure Design

The angle block provides a rigid and massive base for mounting the flexure mechanism. The angle block is clamped to a steel table. The flexure leaves allow for motion in a single degree-of-freedom. The moving platform carries one sample and the normal force assembly holds the other sample. The actuator uses an electromagnet to grab and release the moving platform and a stepper motor and lead screw to position the moving platform.

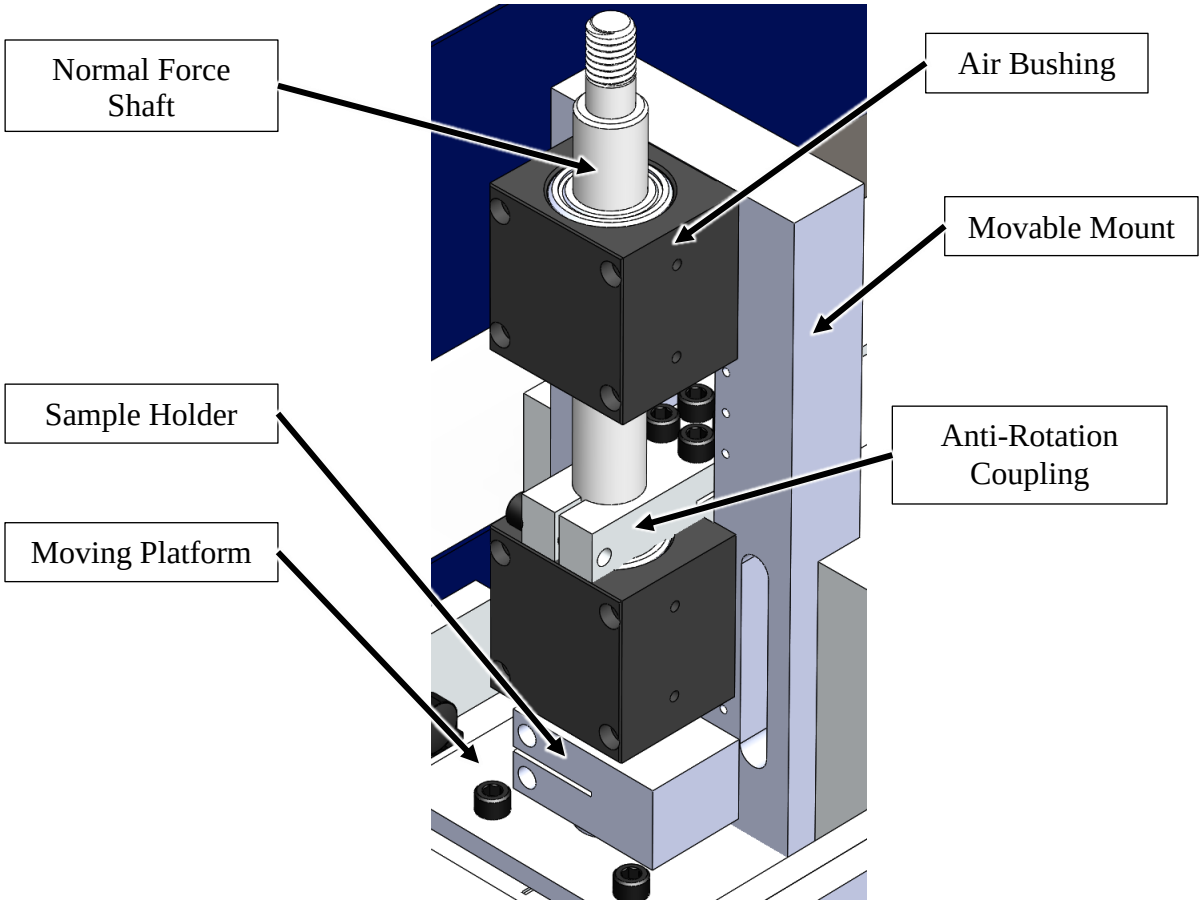

Figure 2: Normal Force Assembly

As seen in Figure 2, air bushings hold the normal force shaft, allowing it to spin and slide vertically, while restricting horizontal motion. To remove to the rotational degree of freedom, the anti-rotation coupling is attached to the shaft on one side and a thin flexure

element on the other side. The sample holder has two independent split clamps. One split clamp attaches to the shaft while the second split clamp holds a 6.35 mm (¼”) diameter sample. The movable mount allows this assembly to move vertically so that different samples can be installed. Figure 3 shows the complete assembly with a single flexure leaf removed for clarity.

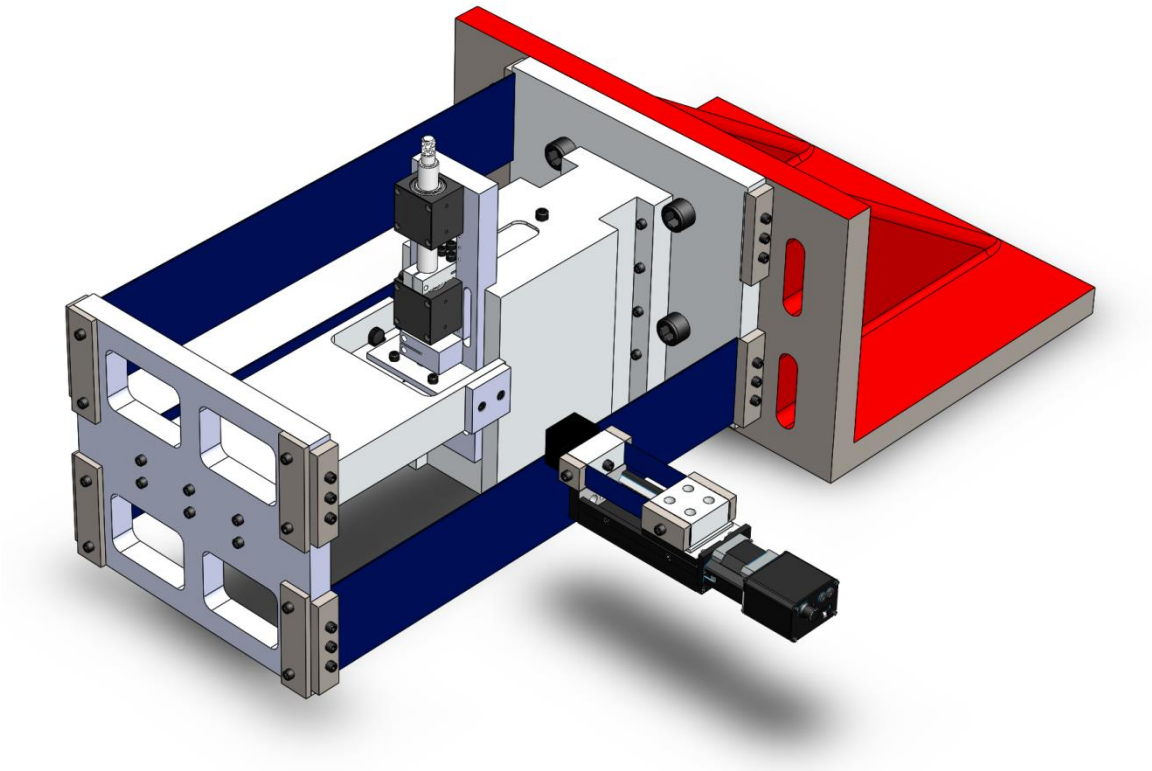

Figure 3: Complete Friction Measurement Assembly

CHAPTER 4: FLEXURE CALCULATIONS

4.1 Flexure Leaf Calculations

The design of the friction measurement machine was based on three major parameters. These include stiffness, range of motion, and (minimized) parasitic motion. These parameters are related to each other by the geometry of the leaves. A graphical approach to selecting the appropriate geometry for the leaves was taken. Increasing the length of the flexure decreases both the stiffness and the parasitic motion, while increasing the range of motion of the flexure. Lengthening the flexures causes the stiffness to decrease which requires the thickness and width of the leaves to increase. The following figures use readily-available thicknesses and widths of 1075 blue tempered spring steel to predict the flexure performance.

For friction testing, a range of motion was chosen for the anticipated experiments. This value was chosen to be 75 mm and then multiplied be a safety factor of 2.

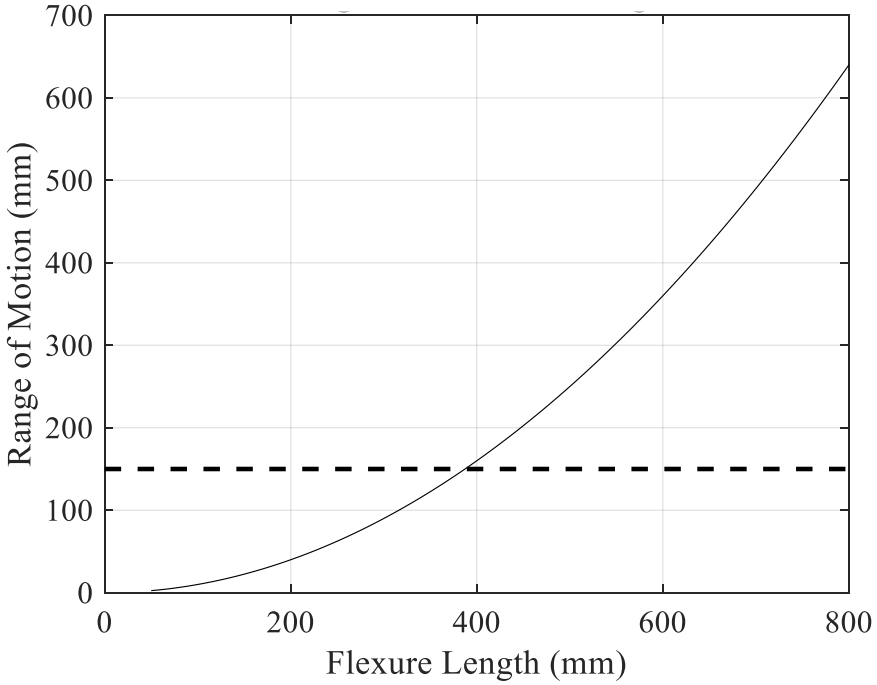

Figure 4: Selection of Flexure Length Dependent Upon Range of Motion

Figure 4 illustrates that a minimum flexure length of 400 mm is necessary to provide the required range of motion. [This figure was generated with the MATLAB code, *Range_and_Parasitic_Motion.m*.] Equation 4.1 was used to determine the range of motion for a given flexure length.

$$x = \frac{\sigma_y L}{3Et} \tag{4.1}$$

where σ_y is the yield strength of the material, L is the length of the leaf, E is the elastic modulus of the material, and t is the thickness of the leaf.

The next parameter that needs must be addressed is the parasitic motion. A maximum parasitic motion value 100 µm was chosen. Equation 4.2 was used to determine the parasitic motion, ∂x, for range of flexure lengths.

$$\partial x = \frac{3x^2}{5L} \tag{4.2}$$

where x is the distance that the flexure has been deflected and L is the length of the flexure leaves. Figure 5 shows the parasitic motion for various flexure lengths. [This figure was generated by the MATLAB code *Range_and_Parasitic_Motion.m*.]

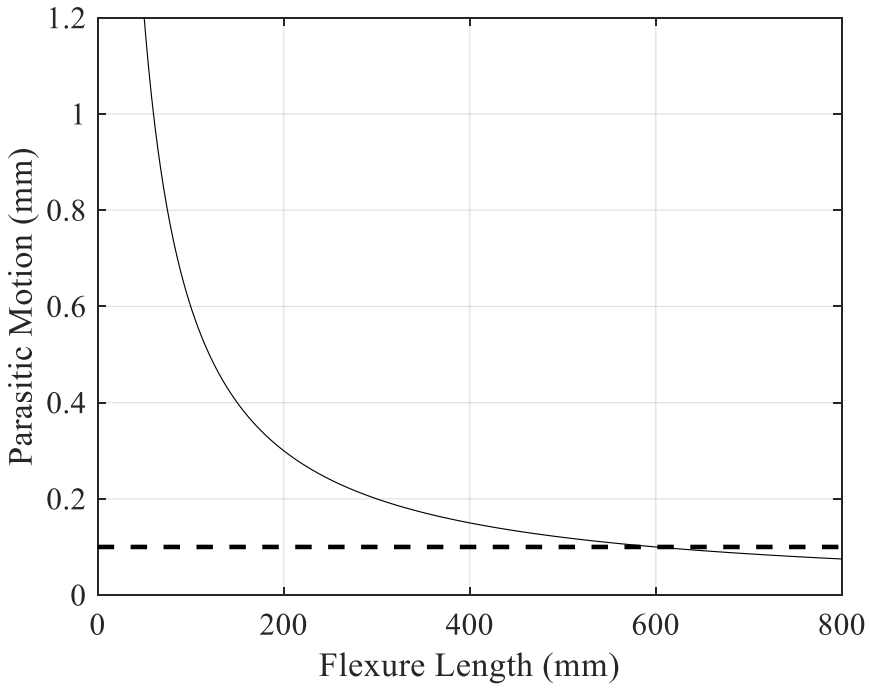

Figure 5: Selection of Flexure Length Dependent Upon Parasitic Motion

A minimum length of 600 mm is required to achieve the desired maximum parasitic motion. This length also meets the criteria described by the previous analysis describing the range of motion. A flexure length of 600 mm is chosen since it meets both criteria.

Given the length, the width and thickness of the flexure leaves need to be selected. The stiffness of the flexure partially determines the natural frequency during free vibration. The next step in the analysis was to determine an appropriate stiffness such that one complete oscillation of the flexure occurs based on an initial displacement of 10 mm. The analysis was performed for a cylindrical sample of diameter 6.35 mm, a Coulomb coefficient of friction of 0.1, and a normal pressure of 2 MPa. Figure 6 shows the results determined using the MATLAB code *Plotting_Friction_Time_Domain.m,* where the stiffness of the machine is changed and the resulting number of oscillations are recorded.

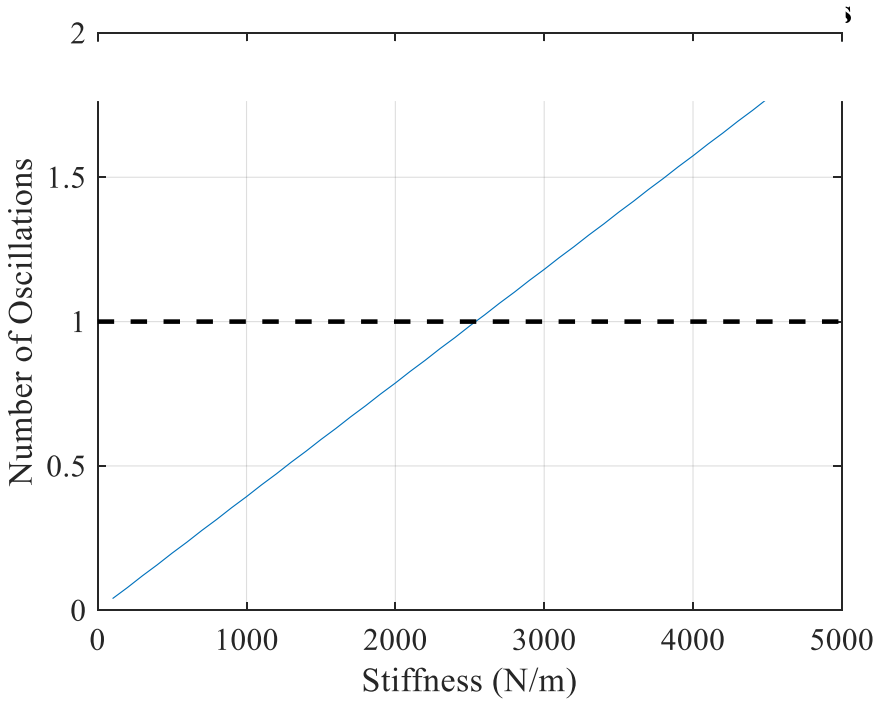

Figure 6: Stiffness Selection Based on Number of Oscillations

Based on the selected parameters, the minimum stiffness to provide a single oscillation is approximately 2500 N/m. Given the values of stiffness and length, the specific size of material can be selected to most closely match these parameters. Various geometries

of blue tempered spring steel were selected and the stiffness for values for each geometry at a length of 600 mm are shown in Figure 7 and Table 1.

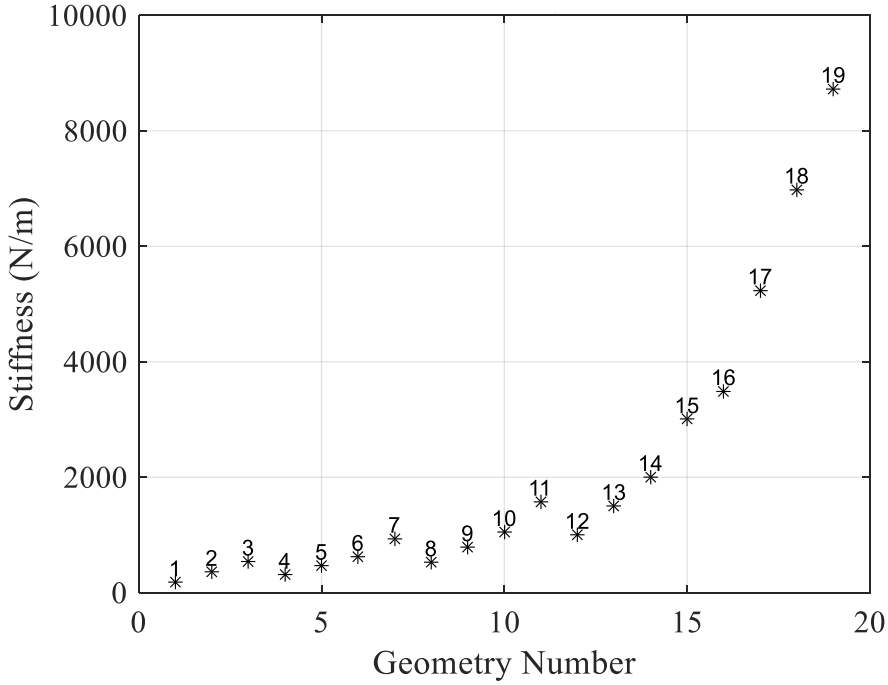

Figure 7: Flexure Geometry Selection Given Length and Target Stiffness

The geometry of the leaf that most closely fits the data is geometry number 14. The width of the flexure is directly correlated to the vertical stiffness of the FMM. The wider the flexure, the higher the stiffness. For this reason, it is beneficial to select a flexure with a width of 101.6 mm (4”) rather than one that is 25.4 mm (1”) wide with the same stiffness. Table 1 shows the different leaf geometries that were analyzed.

Table 1: Flexure Geometry Selection Given Length and Target Stiffness

Geometry Number	Stiffness (N/m)	Thickness (mm)	Width (mm)	Length (mm)
1	180.2	0.89	50.8	600
2	360.4	0.89	101.6	600
3	540.6	0.89	152.4	600
4	311.4	1.07	50.8	600
5	467.1	1.07	76.2	600
6	622.8	1.07	101.6	600
7	934.2	1.07	152.4	600
8	525.4	1.27	50.8	600
9	788.1	1.27	76.2	600
10	1050.7	1.27	101.6	600
11	1576.1	1.27	152.4	600
12	1001.7	1.57	50.8	600
13	1502.5	1.57	76.2	600
14	2003.4	1.57	101.6	600
15	3005.1	1.57	152.4	600
16	3490.9	2.39	50.8	600
17	5236.4	2.39	76.2	600
18	6981.8	2.39	101.6	600
19	8727.3	2.39	127	600

4.2 Air Bearing Stiffness Calculations

Two air bearings are used to support the vertical shaft. The purpose of the bearings is to provide a support with a single degree-of-freedom. The force applied to the sample must remain constant and relative horizontal motion of the sample relative to the vertical shaft must be limited. To estimate the deflection at the sample tip, a simple static beam analysis was conducted for a range of different bearing spacing values. Figure 8 shows the free body diagram of the simply supported normal force shaft.

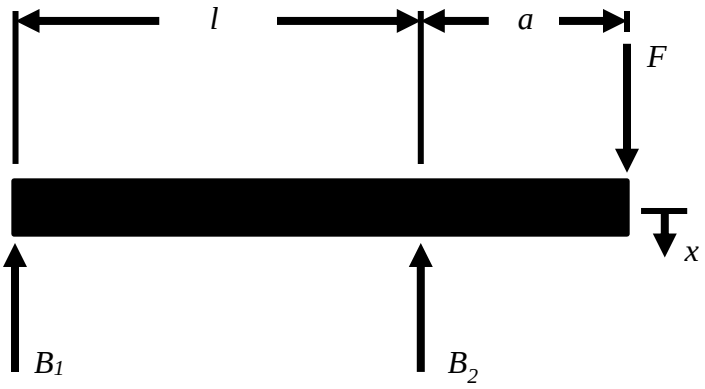

Figure 8: Shaft Deflection Free Body Diagram

This shaft will experience a force that is proportional to the coefficient of friction of the sample and the normal force that is being applied to it (in Figure 8 the normal force is horizontal). Equation 4.1 describes the static deflection of the shaft tip.

$$\Delta x_s = \frac{Fa}{3EI}(al + a^2) \tag{4.1}$$

where Δx_s is the deflection of the beam due to bending, F is the frictional force created between the two material samples, a is stick out distance of the shaft, and l is the center to center spacing of the air bushings. The value of E for the steel shaft is 205 GPa and the value I is based on a circular cross section with a diameter of 12.7 mm (0.5”). The deflection of the shaft at each air bushing is calculated using Equations 4.2a and 4.2b. Equation 4.3 gives the deflection at the tip of the shaft, due to tilting, assuming the shaft is rigid.

$$d_1 = \frac{-aF}{k_{b_1} l} \tag{4.2a}$$

$$d_2 = \frac{aF}{k_{b_2} l + k_{b_2}} \tag{4.2b}$$

$$\Delta x_t = d_2 + \frac{a}{l}(d_2 - d_1) \tag{4.3}$$

where d_1 is the deflection of the top air bushing, d_2 is the deflection of bottom air bushing, k_{b_1} is the stiffness of the top air bushing and k_{b_2} is the stiffness of the bottom air bushing. This analysis uses the reaction forces at the air bearings along with the stiffness of each air bearing to determine the tilt of the shaft when a friction force is applied to the end. In addition to the deflection of the steel shaft, the deflection of the sample that is being tested needs to be considered. The deflection of a 6.35 mm (0.25") diameter cantilever PTFE shaft with a fixed stick out length of 1 mm is added to the deflection of the shaft. The free-body diagram is shown in Figure 9.

Figure 9: Sample Deflection Free-Body Diagram

The deflection of the cantilever sample is calculated using Equation 4.4. Furthermore, the total deflection at the sample tip, including the deflection of the shaft, is represented by Equation 4.5, which is the sum of all the deflections calculated in Equations, 4.1, 4.3, and 4.4.

$$\Delta x_s = \frac{Fs^3}{3EI} \tag{4.4}$$

$$\Delta x_t = \Delta x_b + \Delta x_t + \Delta x_s \tag{4.5}$$

The deflection Δx_t is calculated for a range of bearing spacing values, l. The results from the MATLAB code, *Airbearing_Beam_Deflection.m*, are shown in Figure 10.

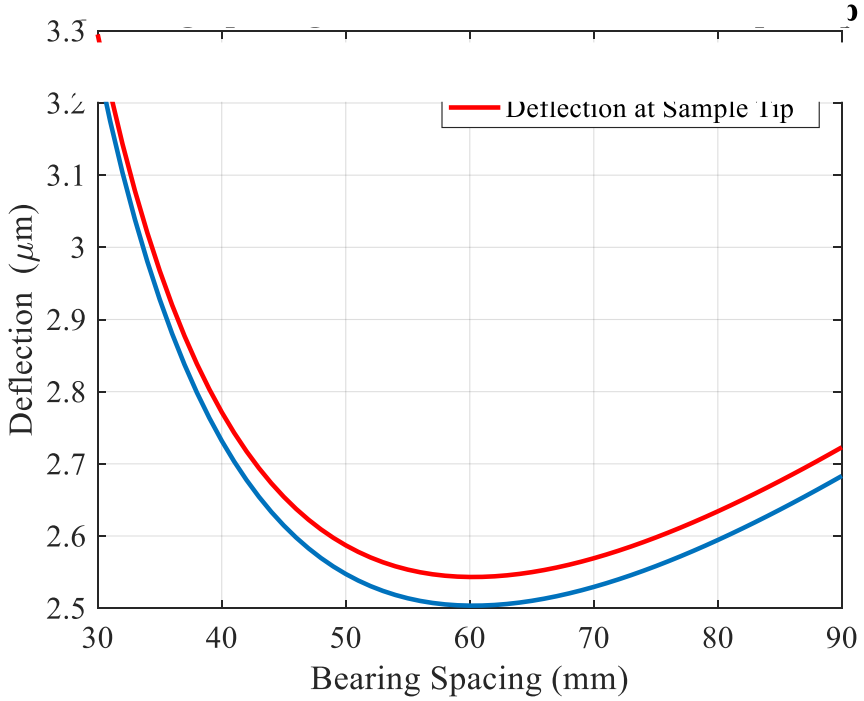

Figure 10: Analysis of 12.7 mm (0.5”) Diameter Shaft to Achieve Minimum Deflection of Sample

The minimum deflection achievable with a shaft diameter of 12.7 mm (0.5”) is approximately 2.55 μm. To reduce the deflection at the tip of the sample the only parameter that can be adjusted is the diameter of the shaft. The shaft size is increased to 19.1 mm (0.75”) and the same analysis is conducted to determine the maximum deflection.

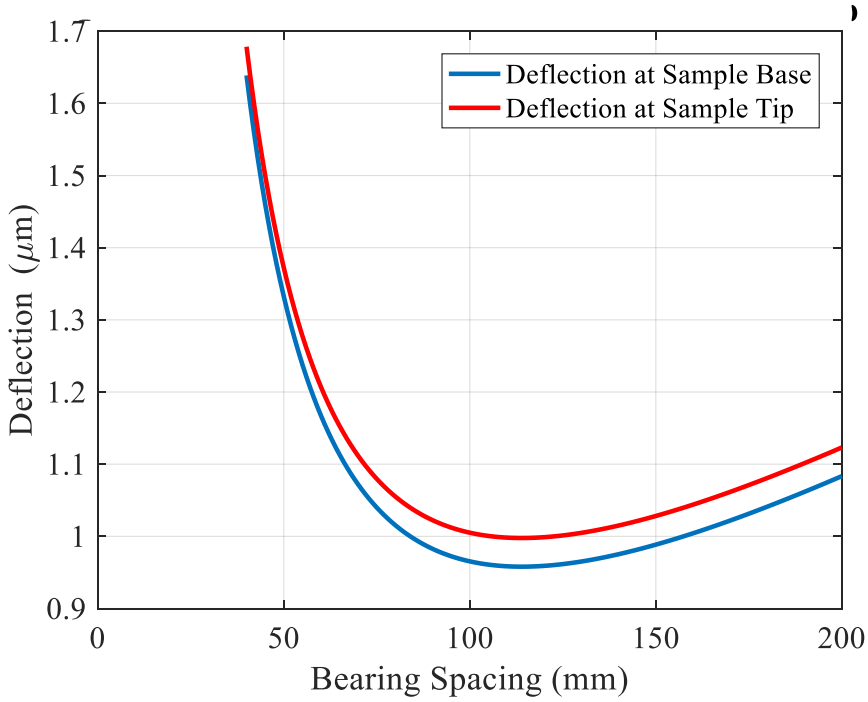

Figure 11: Analysis of 19.1 mm (0.75”) Diameter Shaft to Achieve Minimum Deflection of Sample

Figure 11 presents the optimal bearing spacing of 115 mm. The deflection of the tip of the sample at this location is approximately 1 μm. This deflection is acceptable and the design incorporates a 19.1 mm diameter shaft. Depending on what type of material is mounted to the shaft, the deflection may change as well as the stick out distance.

CHAPTER 5: MANUFACTURING CONSIDERATIONS

The process of manufacturing and assembling the friction measurement machine was taken into consideration. Flexure stops were implemented to assist in the alignment of the flexure leaves. Figure 12 shows the location of these stops.

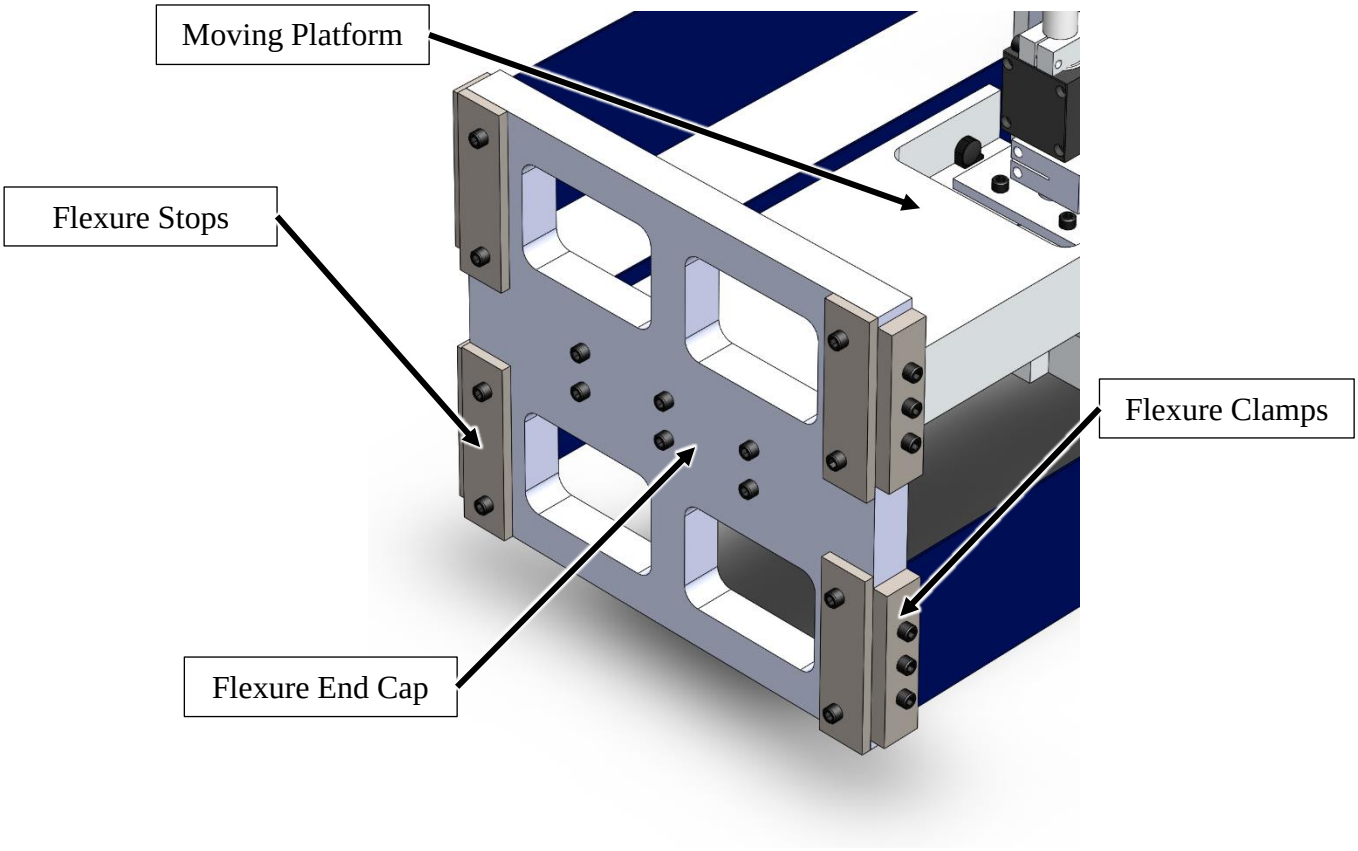

Figure 12: Flexure Stops

The flexure stops are used during the assembly process and provide a reference surface for each leaf to push up against. The flexure leaves are machined to length and, as a result, their relative lengths are sufficiently close such that they can be used in combination with the flexure stops to control the parallelism of the moving platform. The

flexure clamps have a machined section on the side that contacts the flexure leaves to provide two single line contacts. This helps insure that leaf is contacted at the edge of the clamp rather than somewhere in the middle, due to an irregular surface. Figure 13 shows this side of the flexure clamp.

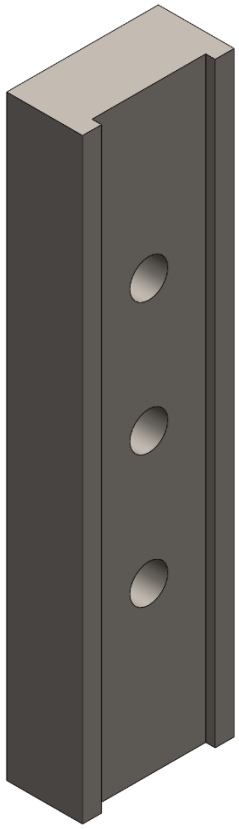

Figure 13: Flexure Clamp

The moving platform was machined with a keyway on it to provide an alignment with the flexure end cap. The flexure end cap has a slot milled into it that mates with this protrusion. The second purpose of this slot is to hold the moving platform while it is being bolted together and support it vertically so that the bolts do not have to support its load. Figure 14 provides an illustration of this slot in the assembly.

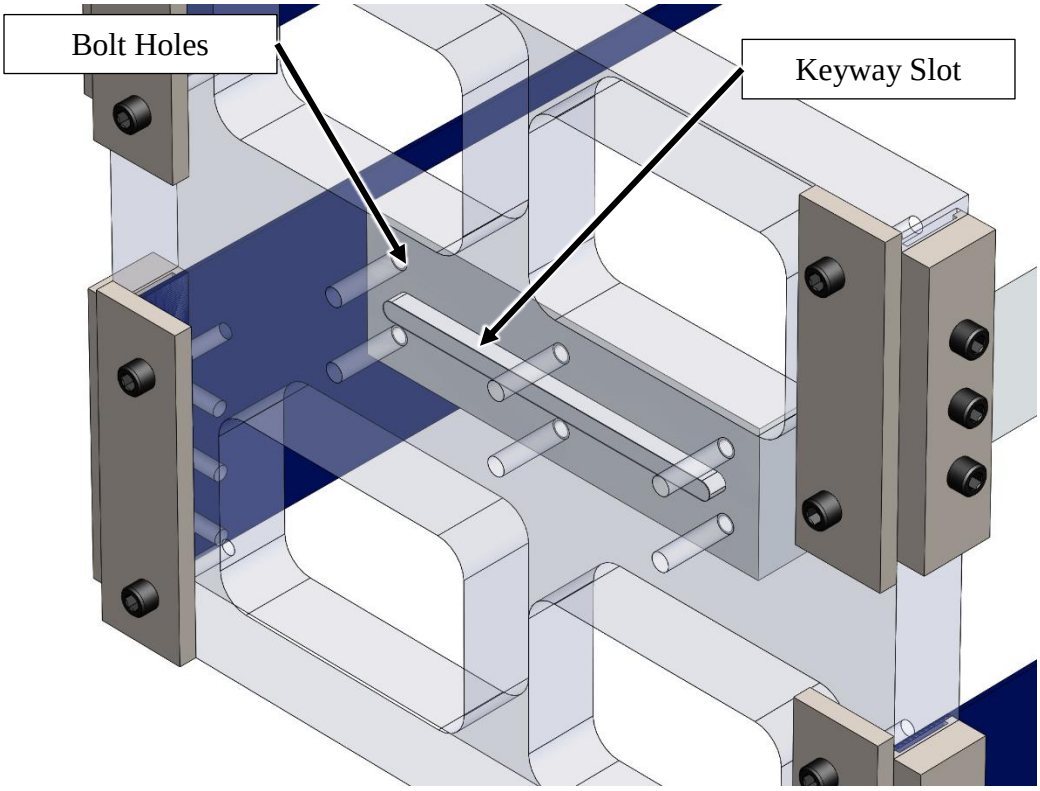

Figure 14: Keyway Slot for Alignment of the Moving Platform

The air bushings are mounted to an aluminum plate that fits in a slot and can move vertically to account for different size samples and alternate attachments in the future. In addition to the assembly being able slide vertically, the air bushing mounts can also move to different locations on the aluminum plate itself for further adjustment. Figure 15 shows the air bushings and accompanying baseplate.

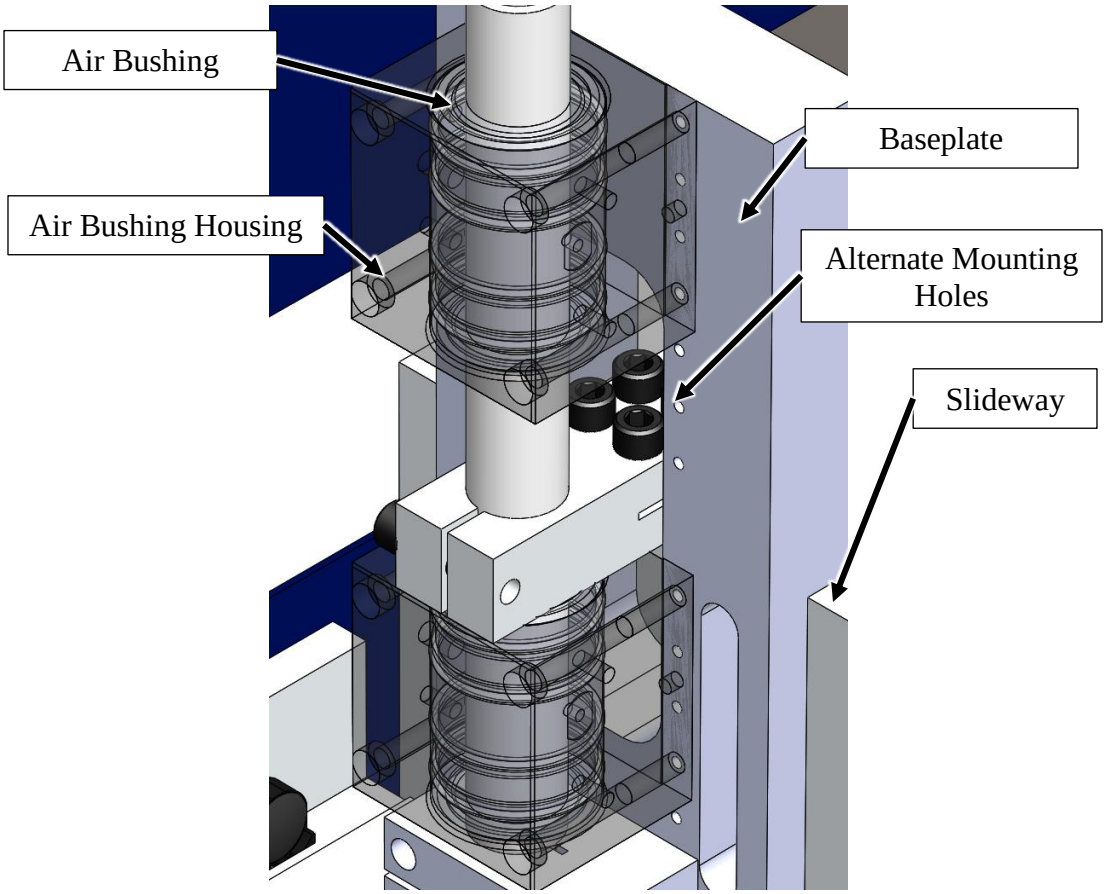

Figure 15: Air Bushing Mounts

Each air bushing resides in a housing that is slightly larger than the air busing itself. Between the air bushing and the housing are two rubber O-rings that support the air bushing. This gives compliance during the assembly process so that two air bushings can be properly aligned. After the shaft is placed in the both air bushings and both housing are secured to the baseplate, the gap between the air bushing and its housing is filled with a rigid, low coefficient of thermal expansion adhesive. This increases stiffness and enables alignment without requiring high machining tolerances.

CHAPTER 6: MACHINE CHARACTERIZATION

6.1 Mass and Stiffness Determination

The simplified model of the FMM used to describe its motion analytically is shown in Figure 16. The model is based on a spring-mass-damper dynamic oscillator, where the moving mass is not equivalent to the normal force.

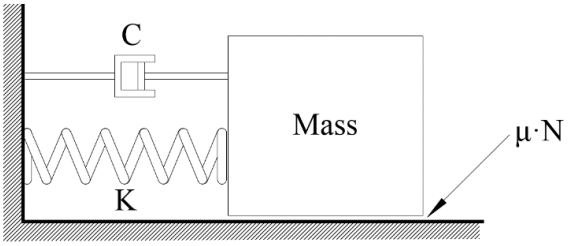

Figure 16: Friction Measurement Simplified Model

Characterizing the mass and stiffness of the FMM is a critical step in defining the friction model. The stiffness and mass parameters are identified through the following procedure. First, multiple masses are selected ranging from 0.9246 grams to 9.716 kg as shown in Table 2.

Table 2: Measured Calibration Masses

Test #	Mass (kg)
1	0.0000
2	0.9246
3	1.9051
4	3.6668
5	4.6279
6	5.4751
7	6.4362
8	8.0597
9	9.7160

For each test number, the corresponding mass is rigidly mounted to the moving platform of the flexure. As shown in Figure 17, the flexure is pulled back to approximately 17 mm and then released under free vibration. The frequency of the flexure loaded with each respective mass is calculated using a peak picking method. The average time between peaks was calculated and used to determine the frequency.

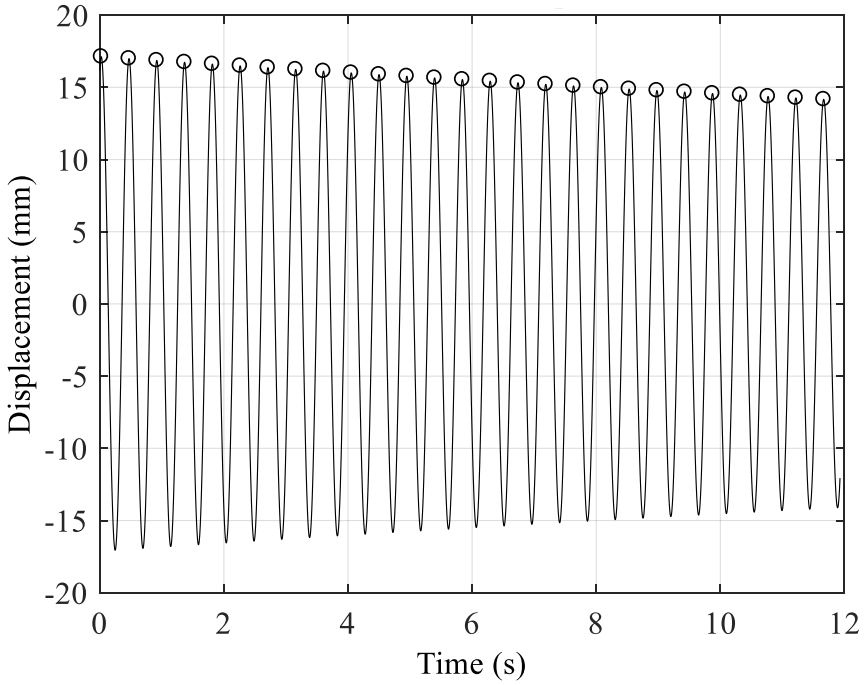

Figure 17: Free Vibration Response of Flexure Loaded With 0.9246 kg

Table 3 shows the results of all 9 tests. As the mass added to the flexure increases, the natural frequency decreases. This is expected since it is known that the natural frequency of can be calculated using Equation 6.1.

Table 3: Frequency Results of Mass Determination Test

Mass (kg)	Frequency (rad/s)
0.0000	14.036
0.9246	13.413
1.9051	12.849
3.6668	11.971
4.6279	11.568
5.4751	11.241
6.4362	10.904
8.0597	10.389
9.7160	9.936

Using Equation 6.1 and replacing the mass term with two variables, one which represents the mass of the flexure, and one that represents the added mass gives Equation 6.2.

$$\omega_n = \sqrt{\frac{k}{m_p}} \tag{6.1}$$

$$\omega_n = \sqrt{\frac{k}{m_p + m_a}} \tag{6.2}$$

where ω_n is the (undamped) natural frequency (rad/s), k is the stiffness of the flexure (N/m), m is the total mass (kg), m_p is the moving platform mass (kg), and m_a is the added mass (kg). A least squares curve fit of the form shown in Equation 6.2 was used to determine m_p and k since ω_n and m_a are measured. The stiffness of the flexure was determined to be $1926\ \mathrm{N/m}$ and the mass of the moving platform was 9.773 kg.

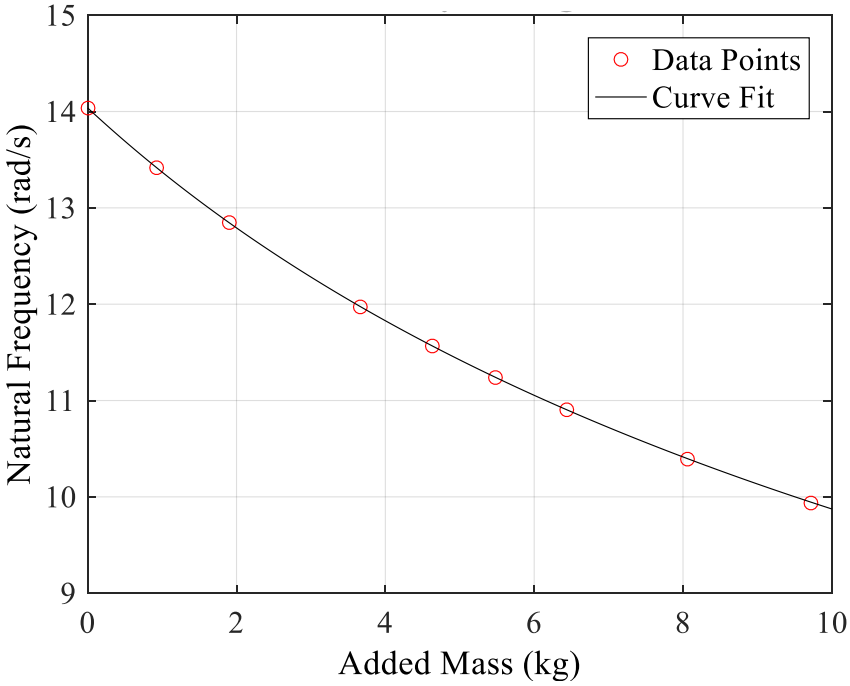

Figure 18: Curve Fit of Mass and Frequency to Equation 6.2

6.2 Force Probe and DMI Stiffness Calculation and Monte Carlo Uncertainty

In addition to calculating the stiffness of the flexure using natural frequency and mass loading, the stiffness is measured using the DMI and a force gage. The DMI is set to zero at the flexure's neutral position. The force gage is mounted to a linear stage which incrementally moves the flexure and measures the reaction force at multiple locations. Figure 19 shows the results.

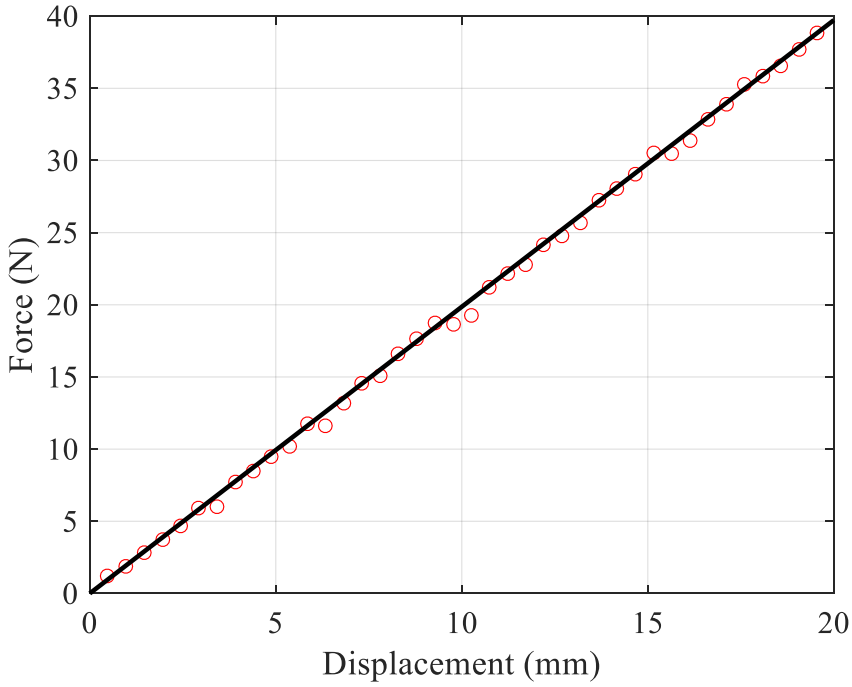

Figure 19: Stiffness Measurement with Force Gage and DMI

Fitting a best fit line to the data gives an approximation of the stiffness of 1985 N/m. The force gage and the DMI each have uncertainties. The DMI error sources include misalignment of the laser with measurement axis, humidity, temperature, and pressure. The force probe has a stated uncertainty of ± 0.15 N from the manufacturer. Performing a Monte-Carlo simulation with these uncertainties and the data taken from the force gage and DMI provide results shown in Figure 20.

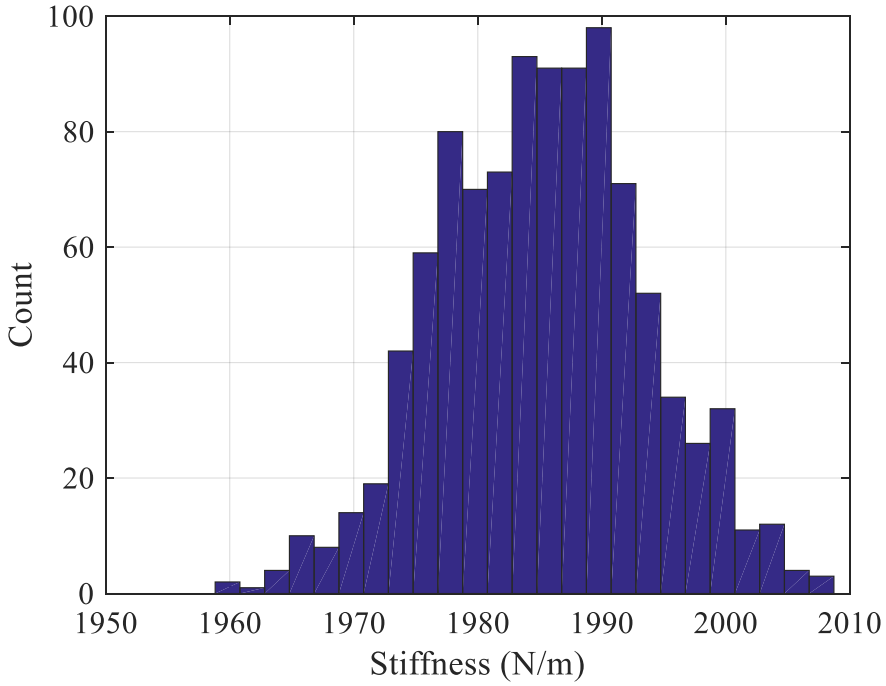

Figure 20: Monte Carlo Stiffness Simulation with Laser Interferometer and Force Gage

The uncertainty of stiffness measured by the force probe and DMI is on the order of ±20 N/m. The added mass and force measurement stiffness identification methods agreed to within 3% (1926 N/m and 1985 N/m).

6.3 DMI Noise When Loaded and Unloaded

Air currents and vibrations in the room can be minimized through careful environmental design. To characterize the FMM noise under steady-state conditions the displacement of the flexure is measured with the DMI. In theory, the data should remain constant over the duration that the test is being performed. Figure 21 shows free vibration measurements with no friction contact.

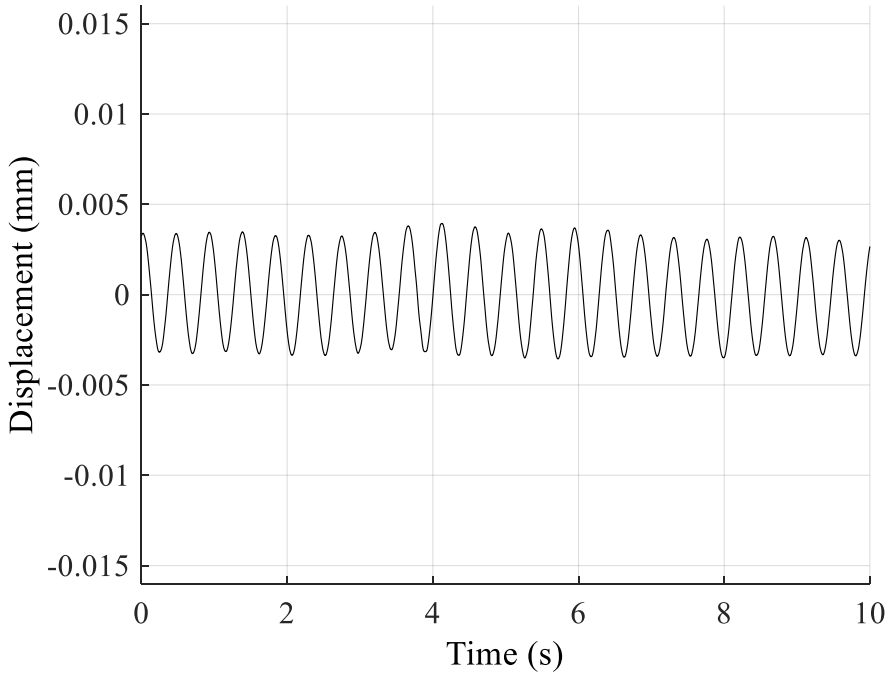

Figure 21: Flexure Noise with No Friction Contact

After the flexure has settled out to equilibrium, the amplitude of noise generated by the environment is approximately 3 μm. The same test is performed except this time a static load, generated by the shaft passing through air bushings, is applied to the moving platform (i.e., a friction contact is included). This test helps to distinguish the magnitude of the noise generated from air currents and local vibrations from the noise accumulated along the measurement path of the laser. Figure 22 shows the results with the friction contact in place.

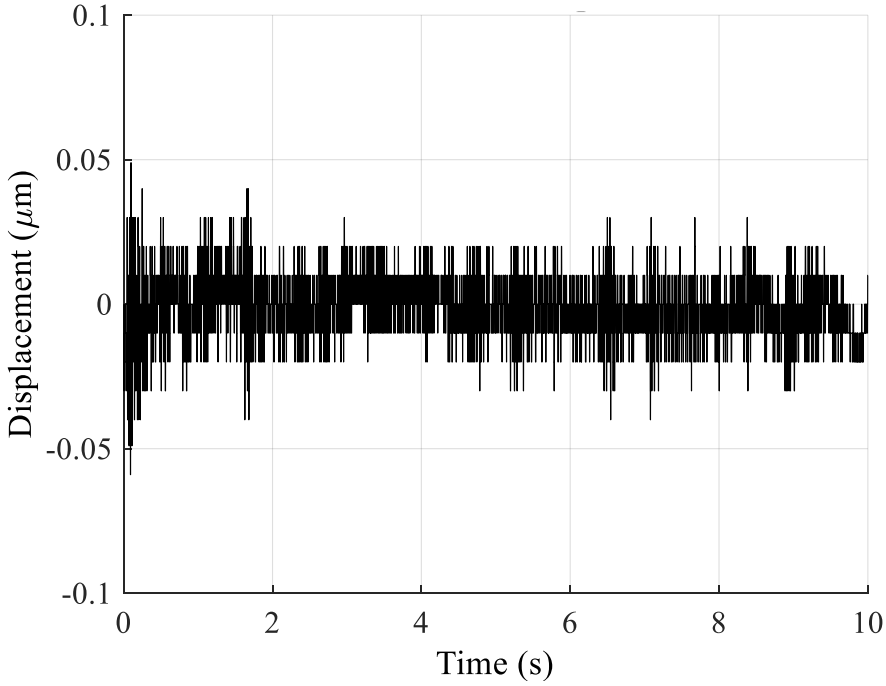

Figure 22: Flexure Noise Loaded by Normal Force Shaft

The noise under these conditions is much less than without the friction contact. An amplitude of approximately 30 nm is observed over the duration of 10 seconds. This noise will be relatively more important when testing very low coefficient of friction contact pairs.

6.4 Characterization of Viscous Damping

Although the viscous damping of the FMM structure is very small, the characterization of friction requires knowledge of the damping ratio present in the structure. The first step in characterizing the friction begins by separating viscous damping from frictional energy dissipation. By measuring the viscous damping in the structure during free vibration with no friction contact, this damping value can be included in the structural dynamics model included in the selected friction model. Figure 23 shows a free vibration response of the FMM. [It was generated using the MATLAB code, *Damping_Determination.m*. This code also calculates the logarithmic decrement and damping ratio of the free vibration.]

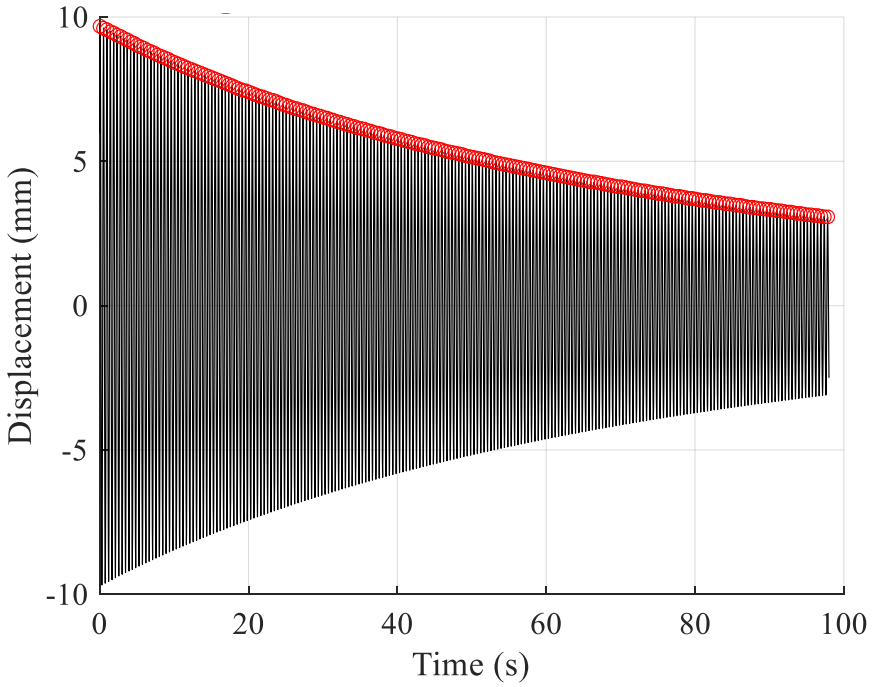

Figure 23: Logarithmic Decrement Damping Calculation for Free Vibration with an Initial Displacement of 9.67 mm and No Friction Contact

The damping ratio can be calculated using the logarithmic decrement. Equation 6.3 defines the logarithmic decrement, δ.

$$\delta = \frac{1}{n} \ln \frac{x(i)}{x(i+n)} \tag{6.3}$$

where n is the number of periods between the two data points, i is the index of the first data point, $x(i)$ is the amplitude of the i^{th} peak, and $x(i+n)$ is the amplitude of the $(n+i)^{th}$ peak. After the logarithmic decrement has been determined, Equation 6.4 calculates the viscous damping ratio, ζ.

$$\zeta = \frac{1}{\sqrt{1 + \left(\frac{2\pi}{\delta}\right)^2}} \tag{6.4}$$

Several tests were completed and the average damping ratio for the FMM was calculated to be 0.00085. This damping ratio is included in the following equation to estimate the dynamic coefficient of friction. In Equation 6.5 all variables are known except for the Coulomb friction coefficient, μ, which can be determined from least-squares fitting. Figure 24 displays the curve fit to the free vibration using Equation 6.5.

$$x(t) = \left(\frac{2\mu N}{m\pi\zeta\,\omega_n^2} + x_o\right) e^{-\zeta w_n t} - \frac{2\mu N}{m\pi\zeta\,\omega_n^2} \tag{6.5}$$

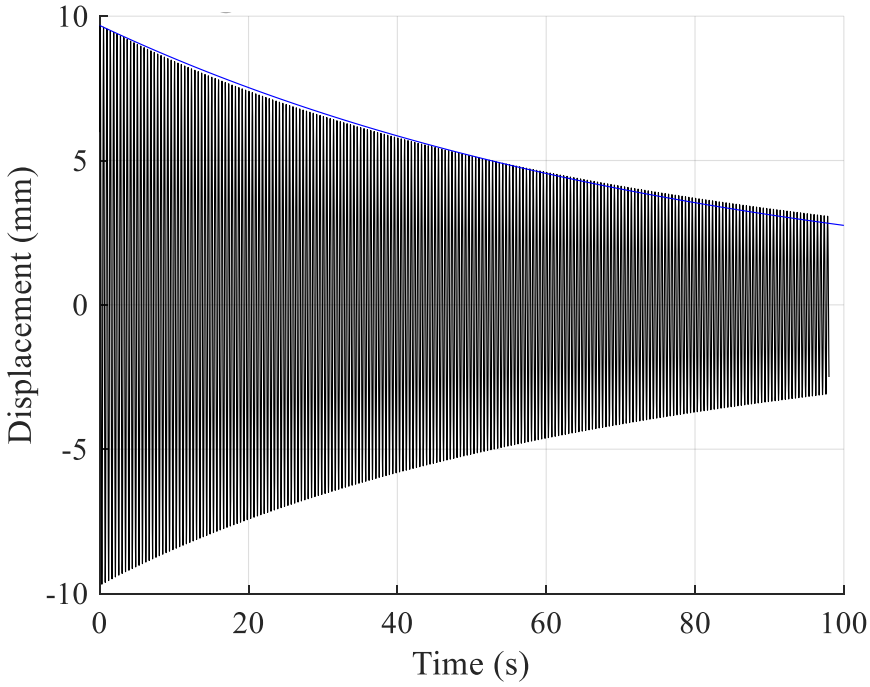

Figure 24: Logarithmic Decrement Best-Fit Curve and Time Domain Free Vibration

CHAPTER 7: CONTROL OF FMM AND SAMPLE PREPARATION

7.1 Control of FMM Through Linear Actuator

Controlling the FMM through a software interface is required to provide a repeatable control method for testing. A linear stage actuated by a stepper motor is used to pull the flexure to its initial displacement point as shown in Figure 25. In addition to the linear stage, an electromagnet is utilized to grab and release the moving platform.

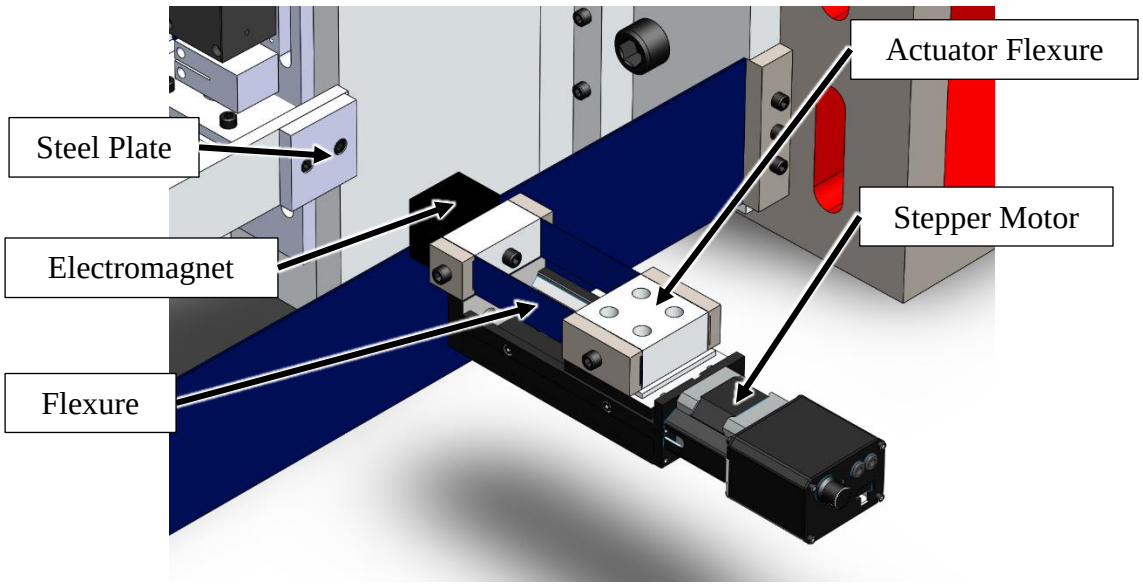

Figure 25: Linear Stage with Stepper Motor Actuator

As the moving platform is pulled to its initial position the parasitic motion must be considered. The flexure between the linear stage and the electromagnet allows for side-to-side motion of the electromagnet and accommodates the small parasitic motion. The stepper motor is controlled through a MATLAB graphical user interface (GUI).

7.2 Graphical User Interface

The GUI was developed to provide preset test routines that include repeatability testing and incremental step size testing. Figure 26 shows the user interface.

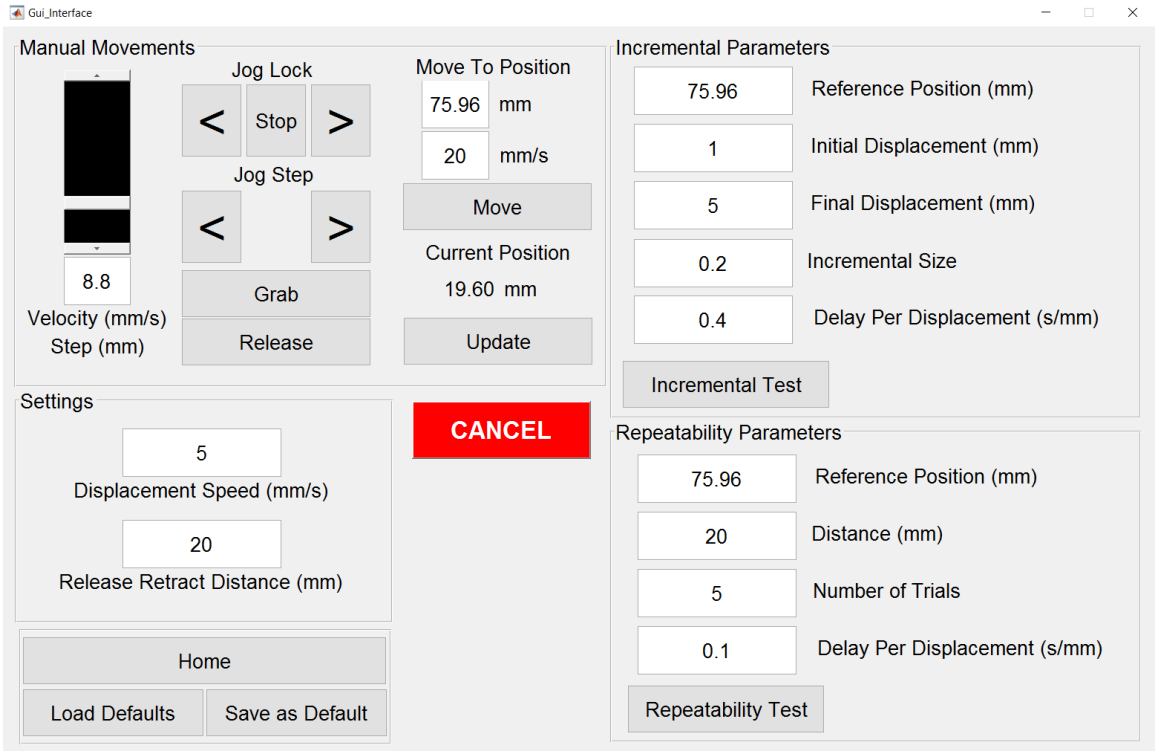

Figure 26: GUI Screenshot

Details of the friction measurement machine control, sample preparation, and testing procedure are included in the user manual (see Appendix B).

CHAPTER 8: CONCLUSIONS AND FUTURE WORK

8.1 Completed Work

A friction measurement machine (FMM) was designed that is based on displacement, rather than force, measurement. The FMM was characterized through various methods to determine the stiffness, damping ratio, range of motion, natural frequency, and modal mass. The user interface and accompanying actuators were developed to provide a user-friendly graphical interface to the machine. Preliminary tests were performed to test the feasibility of the machine. The natural frequency was measured to be 2.24 Hz in free vibration tests. The stiffness was measured to be 1926 N/m and 1985 N/m using the two methods described in sections 6.1 and 6.2, respectively. The damping ratio was calculated to be 0.00085 using the logarithmic decrement as described in section 6.4 Recommendations for improving certain aspects of the measurement loop are included in the following section.

8.2 Future Work

Future improvements, such as various types of sample holders and mounting interfaces, can be developed to adapt the FMM to perform different measurements. The measurement of energy loss due to motion of cables and cable carriers, if included, can also be considered. In addition to measuring frictional energy loss for different interface combinations, future work may include qualification of various sensors such as force transducers.

REFERENCES

[4] P. Dahl. *A solid friction model. Technical Report TOR-0158(3107-18)-1,* The Aerospace Corporation, El Segundo, CA, 1968.

[5] D. A. Haessig and B. Friedland. *On the modelling and simulation of friction.* J Dyn Syst Meas Control Trans ASME, September 1991.

[6] C. Canudas de Wit, Henrik Olsson, K.J., Åström, and P. Lischinsky. *A new model for control of systems with friction,* 40(3) 1995.

[7] Olsson, H., Åström, K.J., Canudas de Wit, C., Gäfvert, M., and Lischinsky, P. *Friction models and friction compensation,* European Journal of Control, 1998

[8] Schmitz, T., Action, J., Ziegert, J., and Sawyer, W.G., *On the difficulty at measuring low friction: Uncertainty analysis for friction coefficient measurements,* Journal of Tribology, 2005

[1] T. Schmitz, C. Evans, A. Davies, and W. Estler. *Displacement Uncertainty in Interferometric Radius Measurements*, CIRP Annals - Manufacturing Technology, 51(1) 2002, Pages 451-454.

[2] S. Smith. *Flexures: Elements of Elastic Mechanisms*, Gordon and Breach, Philadelphia, PA, 2000.

[3] T. Schmitz and S. Smith. *Mechanical Vibrations: Modeling and Measurement*, Springer, New York, NY, 2012.

APPENDIX A:

MATLAB Code

Airbearing_Beam_Deflection.m

```
clear all;
close all;
clc;

%% Bearing Spacing
a = 0.04:0.001:0.2; %m  (distance from bottom bearing to top bearing)
b = 0.05;          %m  (distance from surface to center of bottom bearing)
k_y_1 = 23e6;      %N/m (Stiffness of bottom air bushing)
k_y_2 = 23e6;      %N/m (Stiffness of top air bushing)

%% Sample Dimensions
c = 0.001;   %m  (Stickout of sample)
d = 0.00635; %m  (Sample Diameter)

%% Sample Parameters
mu = 0.15;    %    (Approximate friction coefficient being measured)
N = 31.7;     %N   (Normal force)

%% Beam Parameters
diam = 0.75*25.4/1000; %m
length_b = 0.02;

E_b = 205*1e9;   %N/m^2
I_b = pi*(diam/2)^4/4;

%% Calculations
F_3 = N.*mu;  %N  (Friction force)

d_1 = (-(b./a).*F_3)./k_y_1;  %m   (Deflection at the top bearing)
d_2 = ((b./a+1).*F_3)./k_y_2; %m   (Deflection at the bottom bearing)

d_3 = d_2 + (b./a).*(-d_1 + d_2); %deflection due to tilting of shaft
d_5 = (F_3.*b./(3.*E_b.*I_b)).*(a.*b + b.^2); %


I = pi*(d/2)^4/4;
d_4 = F_3*c^3/(3*0.5*1e9*I); %cantilever deflection of sample tip

%  This formula computes deflection at end for a cantilever beam of the
%  total length.  That is not our case.

disp(strcat(num2str(d_4*1e6), ' um Tip Displacement'))
```

```
%% Plotting
plot(a*1000, d_3*1e6+d_5*1e6, 'LineWidth', 2.0)
grid on
set(gca,'FontSize', 14)
xlabel('a (mm)')
ylabel('deflection_3  (um)')

hold on
plot(a*1000, d_3*1e6+d_4*1e6+d_5*1e6, 'r', 'LineWidth', 2.0)
legend('Deflection at Sample Base', 'Deflection at Sample Tip')
```

Plotting_Friction_Time_Domain.m

```
clear all;
close all;
clc;

for j = 1:50
mu = 0.1;
N = 63.5; %Normal Force (N)
m = 10.5; %Moving Mass (kg)
k = j*100; %Stiffness (N/m)
w_n = 14.13; %Natural Freq (rad/s)
x_0 = 10*10^-3; %Initial Displacement (m)

t = 0.001:0.001:3; %Time (s)

x = -(2*mu*N*w_n.*t)/(3.14*k) + x_0;

pos = 0;

for i = 1:3000
   if x(i) <= 0 && pos == 0
       pos = t(i);
   end
end

for i = 1:3000
   if x(i) <=0
      x(i) = 0;
   else
      x(i) = x(i);
   end
end

x = x.*cos(w_n*t);

osc_perc(j) = pos/0.44464206313
end

plot (t,x.*1000)

grid on
xlabel('Time (s)')
ylabel('Displacement (mm)')
title('Time Domain Simulation of Flexure')

set(gca,'FontName','Times New Roman','FontSize',14.0);
```

```
grid on

titles = get(get(gca,'title'),'string');
title(titles,'fontweight','bold')

figure(2)
plot(100:100:5000,osc_perc)

grid on
xlabel('Stiffness (N/m)')
ylabel('Number of Oscillations')
title('Stiffness Selection Based on Number of Oscillations')

set(gca,'FontName','Times New Roman','FontSize',14.0);
grid on

titles = get(get(gca,'title'),'string');
title(titles,'fontweight','bold')

hold on
plot([0 5000],[1 1])
```

Range_and_Parasitic_Motion.m

```
clear all;
close all;
clc;

%% Analytical Equation For Max Range of Motion and Parasitic Motion
 sigma_y = 1; % GPa
 Length = 50:1:800; %mm
 E = 210;  %GPa
 thick = 1.5875; % mm

 max_range = ((sigma_y.*10.^9)*(Length.*10.^-3).^2)./(3*(E*10.^9)*(thick*10.^-
3))*1000;

 parasitic = 3.*10^2./(5.*Length);

 figure(1)
 plot(Length,max_range,'k')
 grid on
xlabel('Flexure Length (mm)')
ylabel('Range of Motion (mm)')
title('Range of Motion vs Length')

set(gca,'FontName','Times New Roman','FontSize',14.0);
grid on
hold on
plot([0 800],[150 150],'k--','LineWidth',2.0)

titles = get(get(gca,'title'),'string')
title(titles,'fontweight','bold')

 figure(2)
 plot(Length,parasitic,'k')

 grid on
xlabel('Flexure Length (mm)')
ylabel('Parasitic Motion (mm)')
title('Parasitic Motion vs Length')

set(gca,'FontName','Times New Roman','FontSize',14.0);
grid on
hold on
plot([0 800],[0.1 0.1],'k--','LineWidth',2.0)

titles = get(get(gca,'title'),'string')
title(titles,'fontweight','bold')
```

Mass_Deterimination.m

```
% Natural Frequency = sqrt(k/m)
clear all;
close all;
clc;

%% Import Data from Test 1
test1 =
importdata('C:\Users\cloma\Desktop\CHRISTIANS_THESIS\Large_
Flexure\DATA\Testing_Flexure\Mass
Determination\freevibration0kg.mat');

time1 = test1(5650:length(test1),1)-test1(5650,1);
displacement1 = test1(5650:length(test1),2);

plot(time1,displacement1)
hold on

[x, y] = findpeaks(displacement1); % Locate the peaks of
the oscillation
plot(y/1000,x,'ro')

for i = 1:length(y)-1
freq_val1(i) = (y(i+1)-y(1))/(1000*i); % Calculate the
natural frequency
end
format long
freq_val1;

frequency_of_test(1) = 1/mean(freq_val1); % Take the
average of all calculated frequencies

clear x y
%% Import Data from Test 2
test2 =
importdata('C:\Users\cloma\Desktop\CHRISTIANS_THESIS\Large_
Flexure\DATA\Testing_Flexure\Mass
Determination\freevibration0_9246kg.mat');

time2 = test2(3156:length(test2),1)-test2(3156,1);
displacement2 = test2(3156:length(test2),2);

figure(2)
plot(time2,displacement2)
hold on
```

```
[x, y] = findpeaks(displacement2); % Locate the peaks of
the oscillation
plot(y/1000,x,'ro')

for i = 1:length(y)-1
freq_val2(i) = (y(i+1)-y(1))/(1000*i);
end
format long
freq_val2;

frequency_of_test(2) = 1/mean(freq_val2);

clear x y
%% Import Data from Test 3
test3 =
importdata('C:\Users\cloma\Desktop\CHRISTIANS_THESIS\Large_
Flexure\DATA\Testing_Flexure\Mass
Determination\freevibration1_9051kg.mat');

time3 = test3(3000:length(test3),1)-test3(3000,1);
displacement3 = test3(3000:length(test3),2);

figure(3)
plot(time3,displacement3)
hold on

[x, y] = findpeaks(displacement3); % Locate the peaks of
the oscillation
plot(y/1000,x,'ro')

for i = 1:length(y)-1
freq_val3(i) = (y(i+1)-y(1))/(1000*i);
end
format long
freq_val3;

frequency_of_test(3) = 1/mean(freq_val3);

clear x y

%% Import Data from Test 4
test4 =
importdata('C:\Users\cloma\Desktop\CHRISTIANS_THESIS\Large_
Flexure\DATA\Testing_Flexure\Mass
Determination\freevibration3_6668kg.mat');
initial_pt = 4700;
```

```
time4 = test4(initial_pt:length(test4),1)-
test4(initial_pt,1);
displacement4 = test4(initial_pt:length(test4),2);

figure(4)
plot(time4,displacement4)
hold on

[x, y] = findpeaks(displacement4); % Locate the peaks of
the oscillation
plot(y/1000,x,'ro')

for i = 1:length(y)-1
freq_val4(i) = (y(i+1)-y(1))/(1000*i);
end
format long
freq_val4;

frequency_of_test(4) = 1/mean(freq_val4);

clear x y
%% Import Data from Test 5
test5 =
importdata('C:\Users\cloma\Desktop\CHRISTIANS_THESIS\Large_
Flexure\DATA\Testing_Flexure\Mass
Determination\freevibration4_6279kg.mat');
initial_pt = 3600;

time5 = test5(initial_pt:length(test5),1)-
test5(initial_pt,1);
displacement5 = test5(initial_pt:length(test5),2);

figure(5)
plot(time5,displacement5)
hold on

[x, y] = findpeaks(displacement5); % Locate the peaks of
the oscillation
plot(y/1000,x,'ro')

for i = 1:length(y)-1
freq_val5(i) = (y(i+1)-y(1))/(1000*i);
end
format long
freq_val5;

frequency_of_test(5) = 1/mean(freq_val5);
```

```
clear x y
%% Import Data from Test 6
test6 =
importdata('C:\Users\cloma\Desktop\CHRISTIANS_THESIS\Large_
Flexure\DATA\Testing_Flexure\Mass
Determination\freevibration5_4751kg.mat');
initial_pt = 3380;

time6 = test6(initial_pt:length(test6),1)-
test6(initial_pt,1);
displacement6 = test6(initial_pt:length(test6),2);

figure(6)
plot(time6,displacement6)
hold on

[x, y] = findpeaks(displacement6); % Locate the peaks of
the oscillation
plot(y/1000,x,'ro')

for i = 1:length(y)-1
freq_val6(i) = (y(i+1)-y(1))/(1000*i);
end
format long
freq_val6;

frequency_of_test(6) = 1/mean(freq_val6);

clear x y
%% Import Data from Test 7
test7 =
importdata('C:\Users\cloma\Desktop\CHRISTIANS_THESIS\Large_
Flexure\DATA\Testing_Flexure\Mass
Determination\freevibration6_4362kg.mat');
initial_pt = 3750;

time7 = test7(initial_pt:length(test7),1)-
test7(initial_pt,1);
displacement7 = test7(initial_pt:length(test7),2);

figure(7)
plot(time7,displacement7)
hold on

[x, y] = findpeaks(displacement7); % Locate the peaks of
the oscillation
```

```
plot(y/1000,x,'ro')

for i = 1:length(y)-1
freq_val7(i) = (y(i+1)-y(1))/(1000*i);
end
format long
freq_val7;

frequency_of_test(7) = 1/mean(freq_val7)

clear x y
%% Import Data from Test 8
test8 =
importdata('C:\Users\cloma\Desktop\CHRISTIANS_THESIS\Large_
Flexure\DATA\Testing_Flexure\Mass
Determination\freevibration8_0597kg.mat');
initial_pt = 2850;

time8 = test8(initial_pt:length(test8),1)-
test8(initial_pt,1);
displacement8 = test8(initial_pt:length(test8),2);

figure(8)
plot(time8,displacement8)
hold on

[x, y] = findpeaks(displacement8); % Locate the peaks of
the oscillation
plot(y/1000,x,'ro')

for i = 1:length(y)-1
freq_val8(i) = (y(i+1)-y(1))/(1000*i);
end
format long
freq_val8;

frequency_of_test(8) = 1/mean(freq_val8)

clear x y
test9 =
importdata('C:\Users\cloma\Desktop\CHRISTIANS_THESIS\Large_
Flexure\DATA\Testing_Flexure\Mass
Determination\freevibration9_716kg.mat');
initial_pt = 1;

time9 = test9(initial_pt:length(test9),1)-
test9(initial_pt,1);
```

```
displacement9 = test9(initial_pt:length(test9),2);

figure(9)
plot(time9,displacement9)
hold on

[x, y] = findpeaks(displacement9); % Locate the peaks of
the oscillation
plot(y/1000,x,'ro')

for i = 1:length(y)-1
freq_val9(i) = (y(i+1)-y(1))/(1000*i);
end
format long
freq_val9;

frequency_of_test(9) = 1/mean(freq_val9)

frequency_of_test = frequency_of_test*2*pi; % Convert to
rad/s

mass = [0 0.9246 1.9051 3.6668 4.6279 5.4751 6.4362 8.0597
9.716]; % Addded Mass

figure(10)
plot(mass, frequency_of_test,'ro') % Plot Results
hold on

x = 0:0.001:10;
y = sqrt(1926./(x+9.773));
plot(x,y,'k')

grid on
set(gca,'FontSize', 14)
xlabel('Added Mass (kg)')
ylabel('Natural Frequency (rad/s)')
title('Mass Determination by Adding Known Masses')
legend('Data Points','Curve Fit')

set(gca,'FontName','Times New Roman','FontSize',14.0);
grid on

titles = get(get(gca,'title'),'string');
title(titles,'fontweight','bold')
```

Damping_Determination.m

```
clear all;
close all;
clc;

%% Logarithmic Decrement

data = importdata('free_intitial10_1.mat');

time = data(2000:length(data),1)-data(2000,1);
displacement = data(2000:length(data),2);


[PKS,LOCS] = findpeaks(displacement); % Find peaks of
oscillation

n = 1; % Span to Measure Logarithmic Decrement
j = 1; % Index Counter

for i = 1:length(PKS)-n % Calculate the damping ratio
    log_dec = (1/n)*log(PKS(i)/PKS(n+i));
    damp_ratio(j) = 1/sqrt((1+(2*pi)/log_dec)^2);
    j = j+1;
end

disp(mean(damp_ratio)); % Calculate the average damping
ratio

figure(1)
hold on
plot(time,displacement,'k')
plot(time(LOCS),PKS,'ro')

set(gca,'FontName','Times New Roman','FontSize',14.0);
grid on

xlabel('Time (s)')
ylabel('Displacement (mm)')
title('Logarithmic Decrement Free Vibration')

titles = get(get(gca,'title'),'string');
title(titles,'fontweight','bold')


%% Plot logarithmic decrement

t = 0.001:0.001:100;
```

```
x_o = 9.679;
w_n = 2.2*(2*pi); % Natural Frequency of Flexure
x = x_o.*exp(-damp_ratio(50).*w_n.*t); %Viscous Damping
Equation

hold on
plot(t,x,'b')
```

APPENDIX B:

User Manual

The graphical user interface, GUI, controls the moving stage and the electromagnet components of the FMM. The GUI consists of four sections: Manual Movements, Incremental Parameters, Repeatability Parameters, and Settings. This GUI has no interaction with the laser interferometer and performs no analysis after the test has completed.

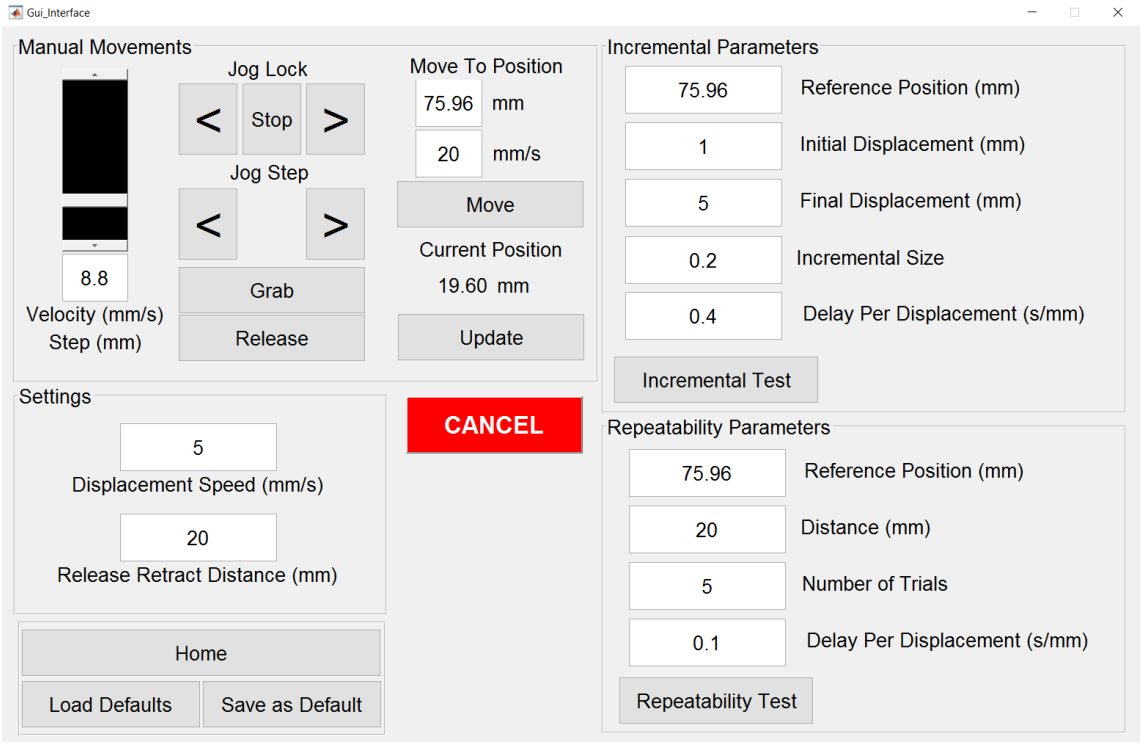

Figure 27: Linear Stage Graphical User Interface

When the GUI is launched via MATLAB, the Arduino board is linked to the computer and the linear stage is homed. Once the stage has reached the home position, the GUI will appear on the screen. If an error occurs or the stage does not home properly, check to make sure both the stage and Arduino components are connected to the computer via USB cable.

Manual Movements

The manual movements section can be used to find the neutral location of the flexure, perform manual tests, and to check the operation of various components. To insure the laser and stage are reading the proper units, the stage can be used to pull back the friction measurement machine a specified distance. The current position should read approximately the same value as the laser interferometer setup.

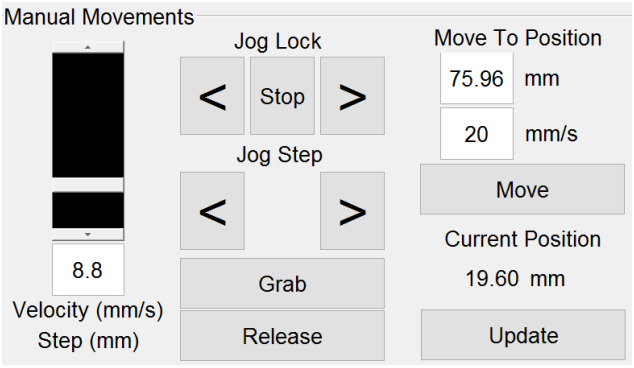

Figure 28: Manual Movements Screenshot

Jog Lock: This button moves the stage in the positive or negative direction at the velocity displayed in the lower left-hand corner.

Jog Step: This button moves the stage in the positive or negative direction the distance displayed in the lower left-hand corner.

Grab: This button turns the electromagnet on

Release: This button reverses the polarity of the electromagnet and then cuts the power to release the flexure

Move: This button moves the stage to the specified absolute position at the specified speed

Update: This button displays the current position in the case the stage was manually moved using the dial on the stage

Selector Bar: Located on the left hand side of this sector, this selector bar adjusts the speed and step size utilized by the jog lock and jog step functions.

Incremental Parameters

An incremental test means that each successive release will be slightly further away from the neutral location of the FMM. The initial and final values, along with the incremental size, are set by the user. The final displacement should not exceed the reference position, as this would be outside the range of the stage.

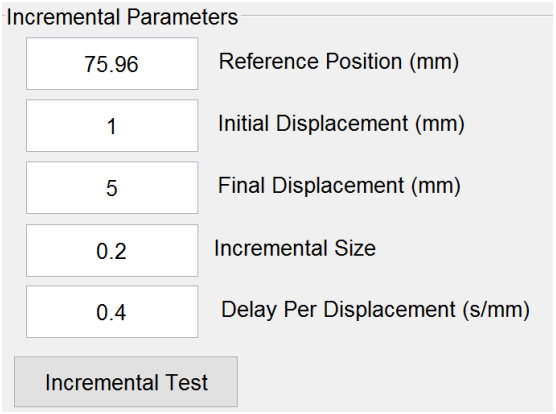

Figure 29: Incremental Parameters Screenshot

Reference Position: This field represents the position of the stage when the FMM is in the neutral position.

Initial Displacement: This field represents the location of first release location relative to the reference position.

Final Displacement: This field represents the location of the final release location relative to the reference position.

Incremental Size: This field represents the incremental distance for each subsequent test. The incremental test will continue until the final displacement is reached.

Delay per Displacement: This field sets the delay time after the electromagnet has been released. The delay time is dependent on the release distance. The delay, in seconds, is equal to the release distance, in mm, times the value entered in this field.

Incremental Test: This button initializes the incremental test.

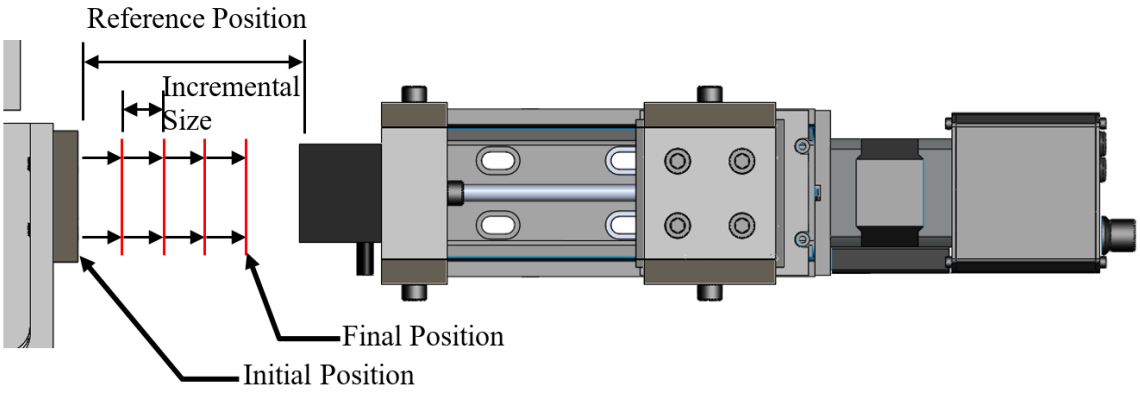

Figure 30: Incremental Physical Representation of Parameters

Repeatability Parameters

The repeatability of the setup can be tested. The stage will go to the same designated release position for the number of trials set by the user.

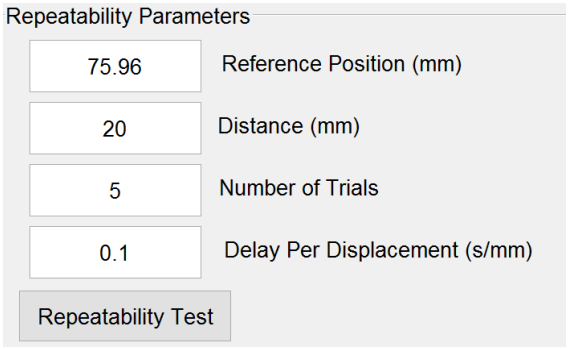

Figure 31: Repeatability Parameters Screenshot

Reference Position: This field represents the position of the stage when the FMM is in the neutral position.

Distance: This field represents the distance relative to the reference position that the stage will move to for every trial.

Number of Trials: This field represents the number of times the stage will pull the FMM back to the specified distance.

Delay per Displacement: This field sets the delay time after the electromagnet has been released. The delay time is dependent on the release distance. The delay, in seconds, is equal to the release distance, in mm, times the value entered in this field.

Repeatability Test: This button initializes the repeatability test.

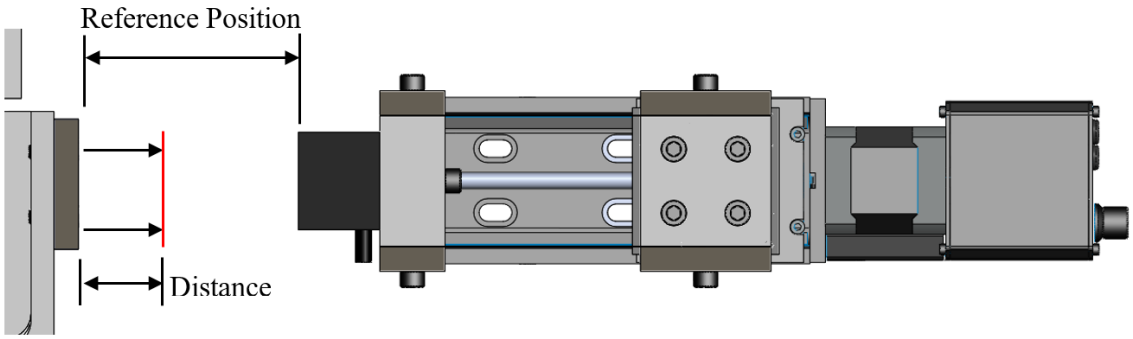

Figure 32: Repeatability Physical Representation of Parameters

Settings

Typically, the settings should only be set once. To ensure that the settings remain saved when the GUI is launched the next time, use the Save as Default button.

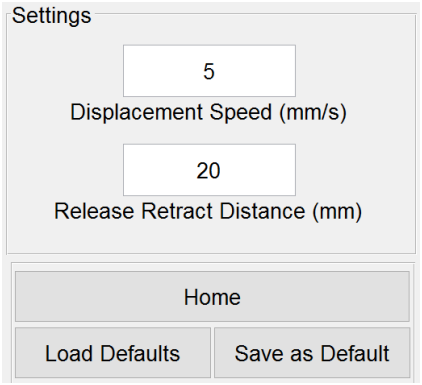

Figure 33: Settings Screenshot

Displacement Speed: This field sets the speed of the stage while moving the FMM to the desired release point.

Release Retract Distance: This field sets the distance the stage will retract after releasing the FMM.

Home: This button homes the stage. This is automatically performed when the GUI is initialized.

Load Defaults: This button loads the previously saved default values for all fields.

Save as Default: This button saves all set parameters as the new default values. These will now be the values that load when the load defaults button is pressed as well as when the GUI is launched.

Laser Interferometer Setup

The measurement system for the FMM is a displacement measuring interferometer. The laser source is an Agilent 5519 A. The beam splitter, HP 10766A, and the retroreflector, HP 10767A, assembly is located on the left side of the FMM, as shown in Figure 34.

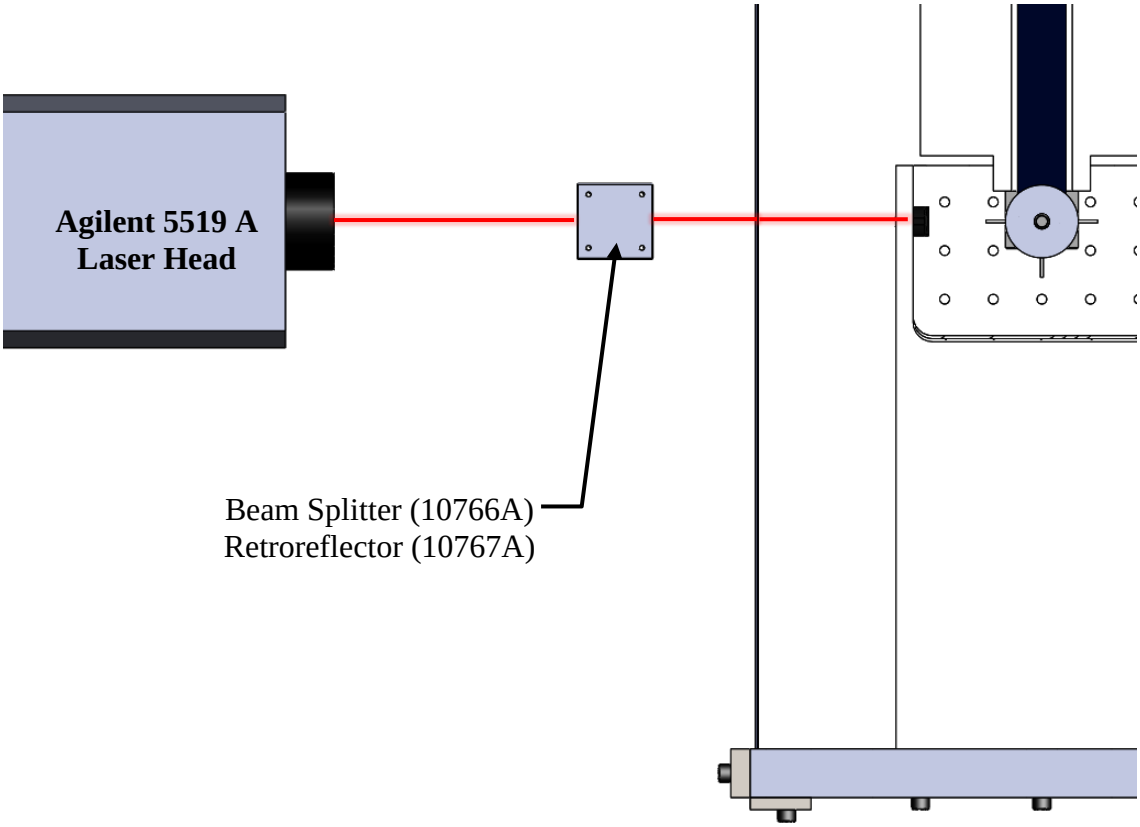

Figure 34: Laser Interferometer Setup

Mechanical Procedure

Turn the laser on using the switch on the back of the laser head. Turn the dial on the front of the laser head to the “straightness” position. Align the laser head with the FMM by aiming the laser into the retroreflector located on the FMM. If the laser head is properly aligned the laser should return to the same hole from which it was emitted. Next, move the FMM platform throughout its range and make sure the laser does not deviate from its original path. If the returning beam shifts, the laser head is not aligned with the motion of the FMM platform. Continue adjusting the laser until the beam no longer shifts.

Place the Beam Splitter and Retroreflector assembly, shown in the Figure 35, in the beam path. Raise or lower the beam splitter so that the returning beam enters the same hole as the exiting beam.

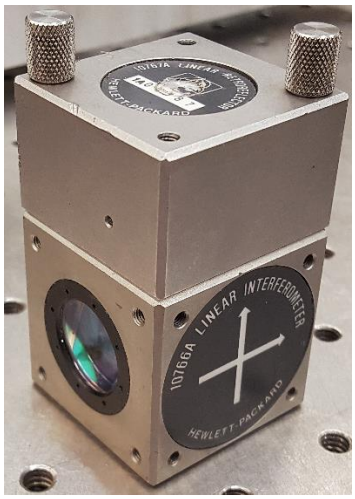

Figure 35: Beam Splitter and Retroreflector Assembly

Software Setup

Launch the software as shown in Figure 36. Prior to launching the software, the laser should be turned on.

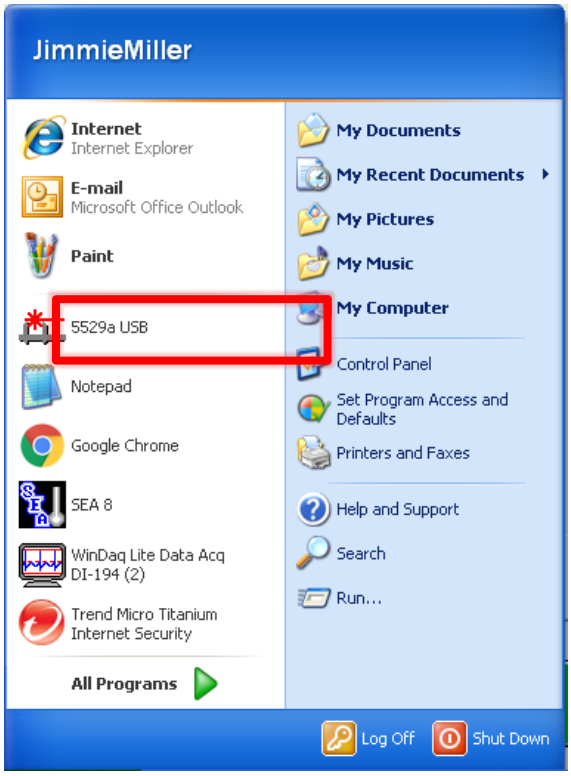

Figure 36: Software Location

The following steps should be followed to prepare the software for recording continuous data. After the software loads click “Other Meas” shown in Figure 37.

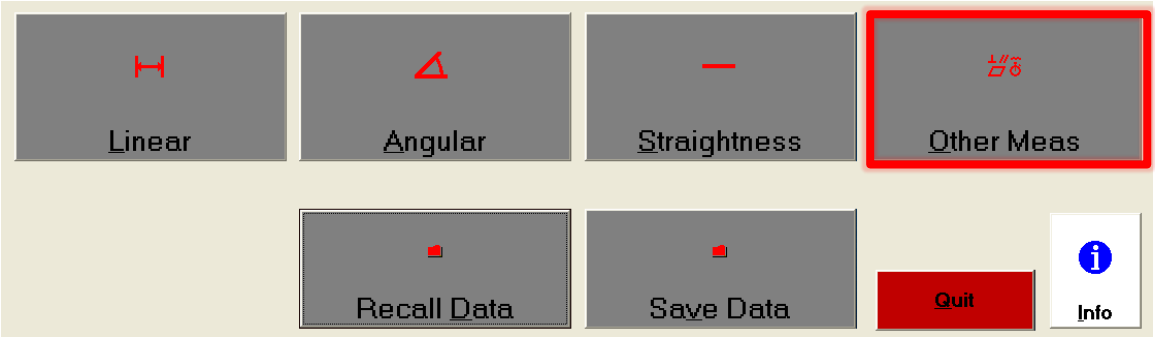

Figure 37: Step 1

Click “Timebase” on the bottom row.

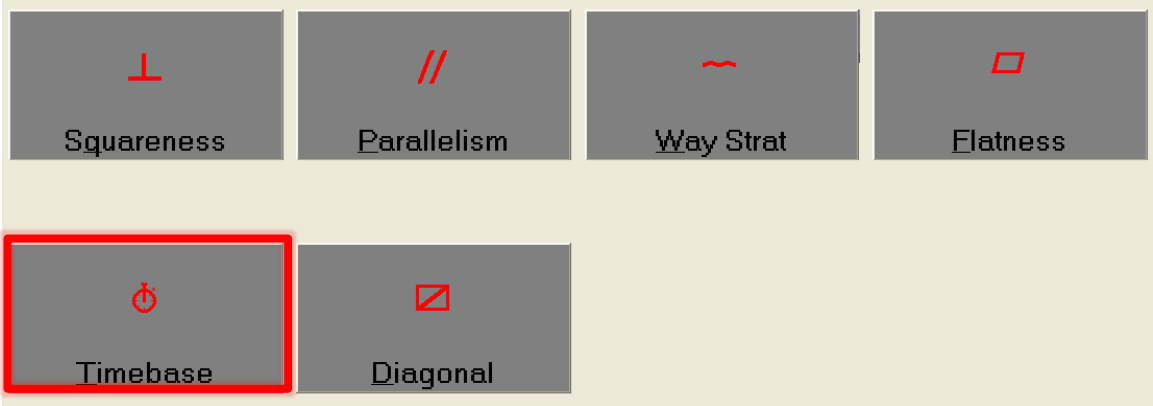

Figure 38: Step 2

On the next screen, if the laser has finished warming up, you will see the current displacement. This is the screen where the laser can be zeroed prior to taking data. Proceed by clicking the “Set Up Meas.” button, shown in Figure 39.

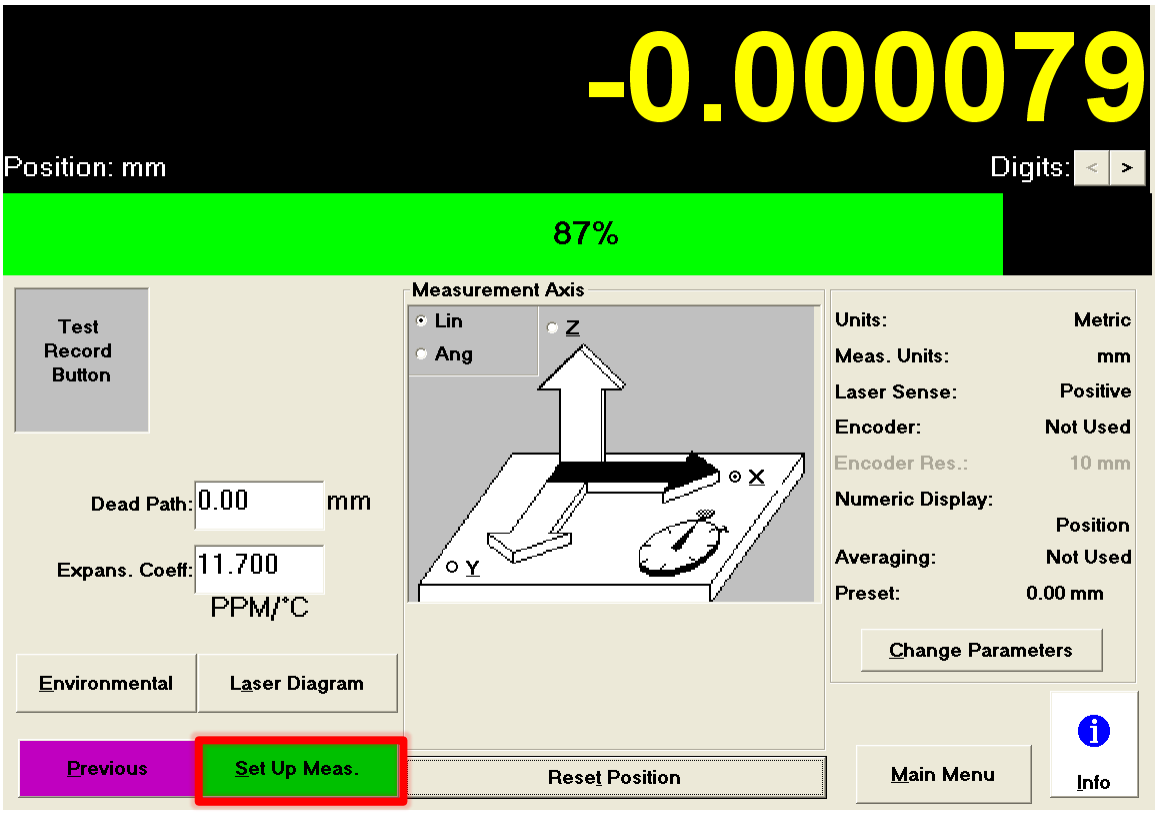

Figure 39: Step 3

The software will only record up to 100,000 data points. First enter the sample interval in seconds. At a sample interval of 0.001 seconds (1000 Hz) the maximum record time is 100 seconds. Be sure to select a sample interval that will give the most data while still being able to record the data for the duration of the test. After the sample interval has been set, select the option “No. of Points” and then fill in the field below according to the test that will be performed.

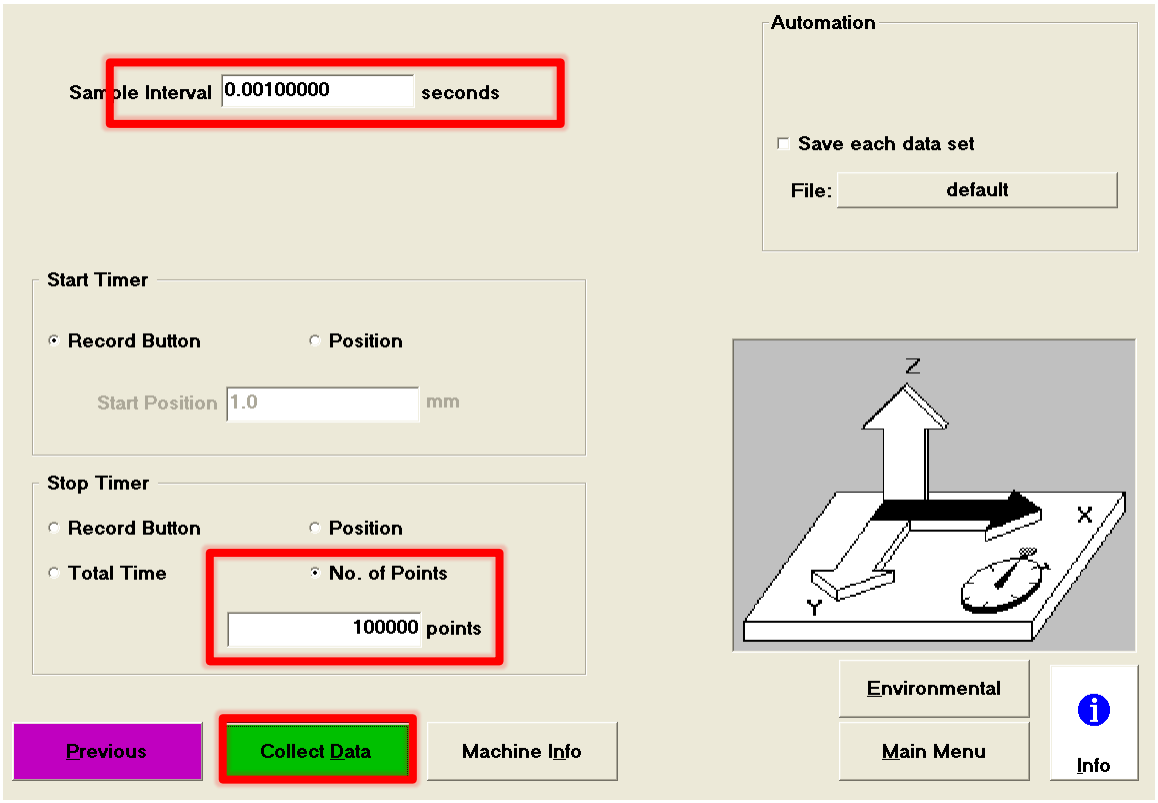

Figure 40: Step 4

When the two settings described previously are specified, click the “Collect Data” button to proceed to the next screen.

When it is time to record data, press the “Arm Timer” button twice. After the first click it will change to a green “Start Timer” button.

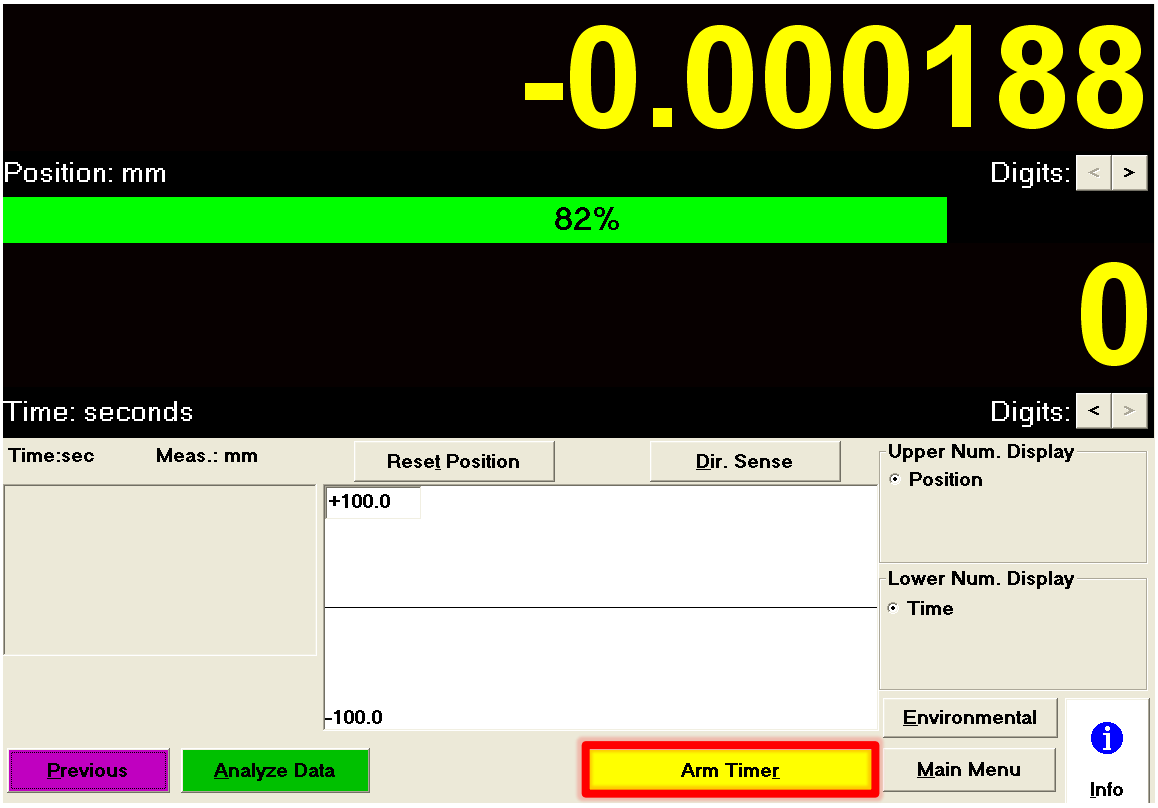

Figure 41: Step 5

If the system is properly taking data you should see a screen that looks very similar to the image in Figure 42. The current position will not be displayed and the timer will show how long it has been since the timer started. When the number of data points that were set in the previous steps have been recorded, the data acquisition will automatically stop. If the test finishes before the number of data points has been reached, clicking the "Stop Timer" button will end the data acquisition and will automatically proceed to the next screen.

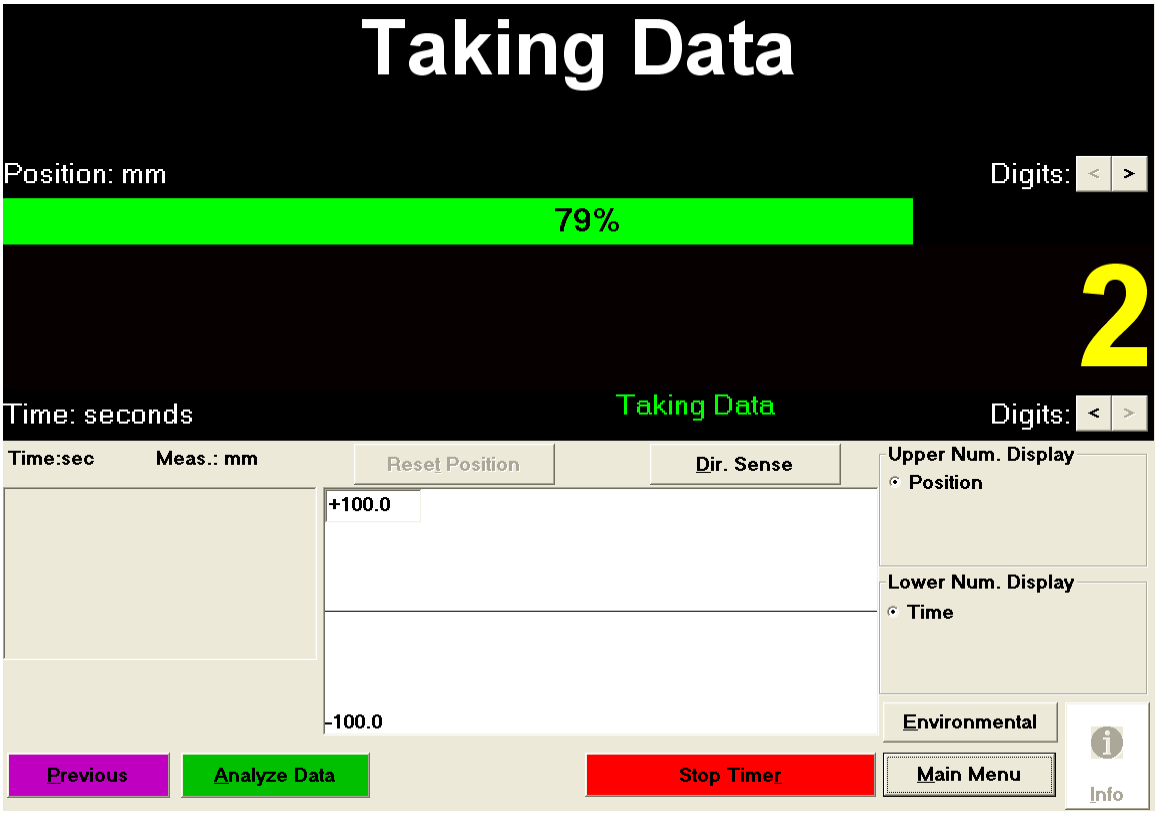

Figure 42: Step 6

When the data acquisition is complete the program will display the data. To save the data, first click the “Show Data” button shown in Figure 43.

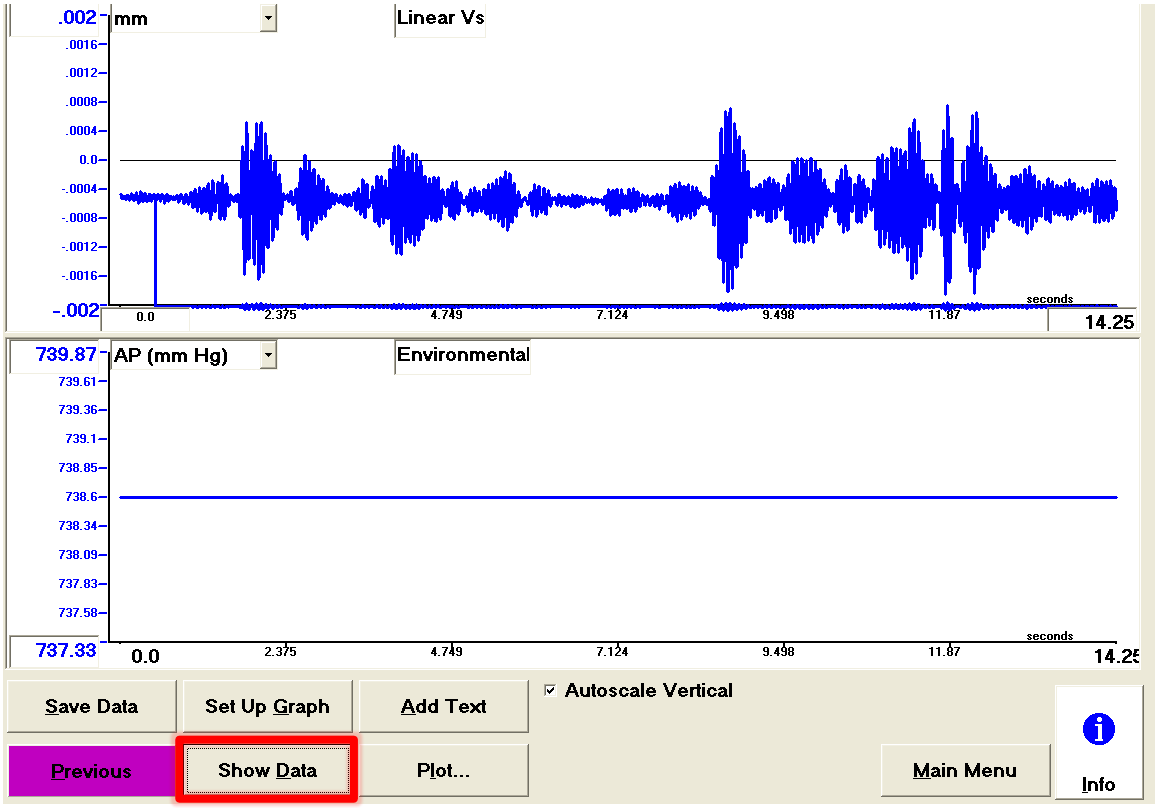

Figure 43: Step 7

The data is now displayed on the right-hand side and to save it to a .txt file click the “Print to File” button.

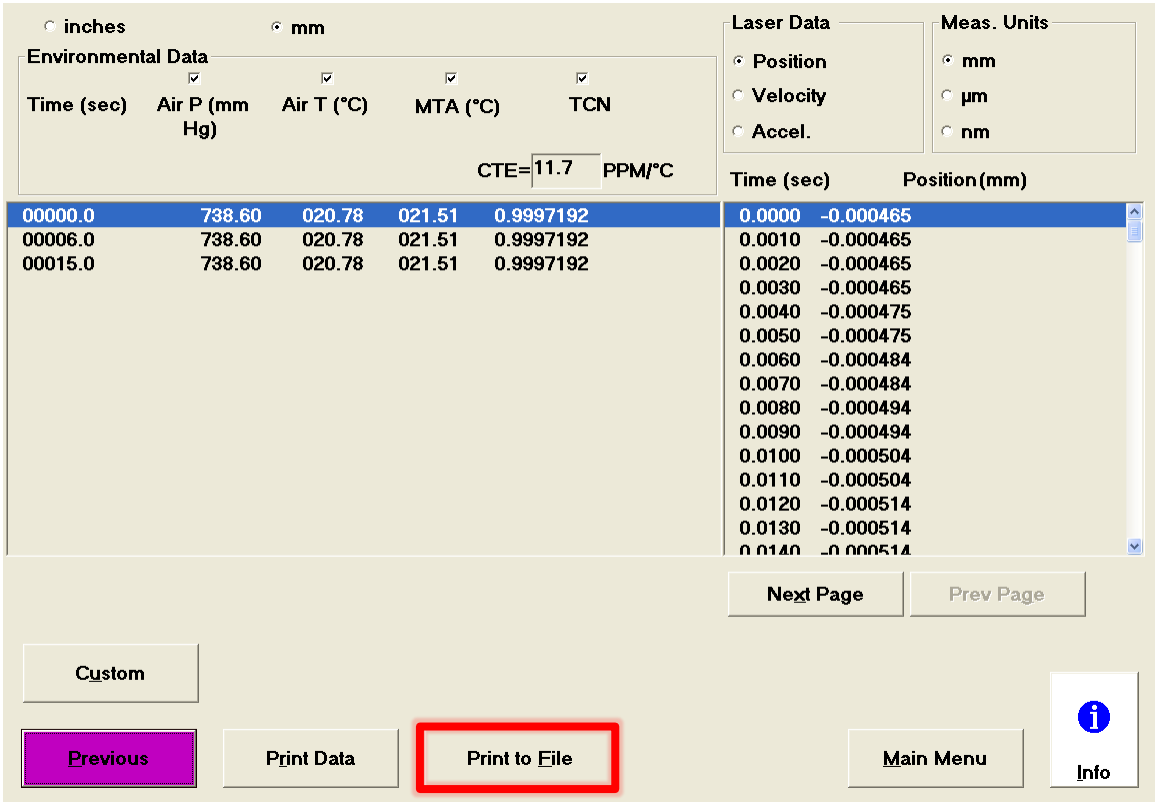

Figure 44: Step 8

Browse through the Directories to find the desired location to save the data to. The first time saving data after the program is launched will require that a ".lin" file is saved. Simply save this file and then proceed by saving the data again. The second time through the filename will show .txt.

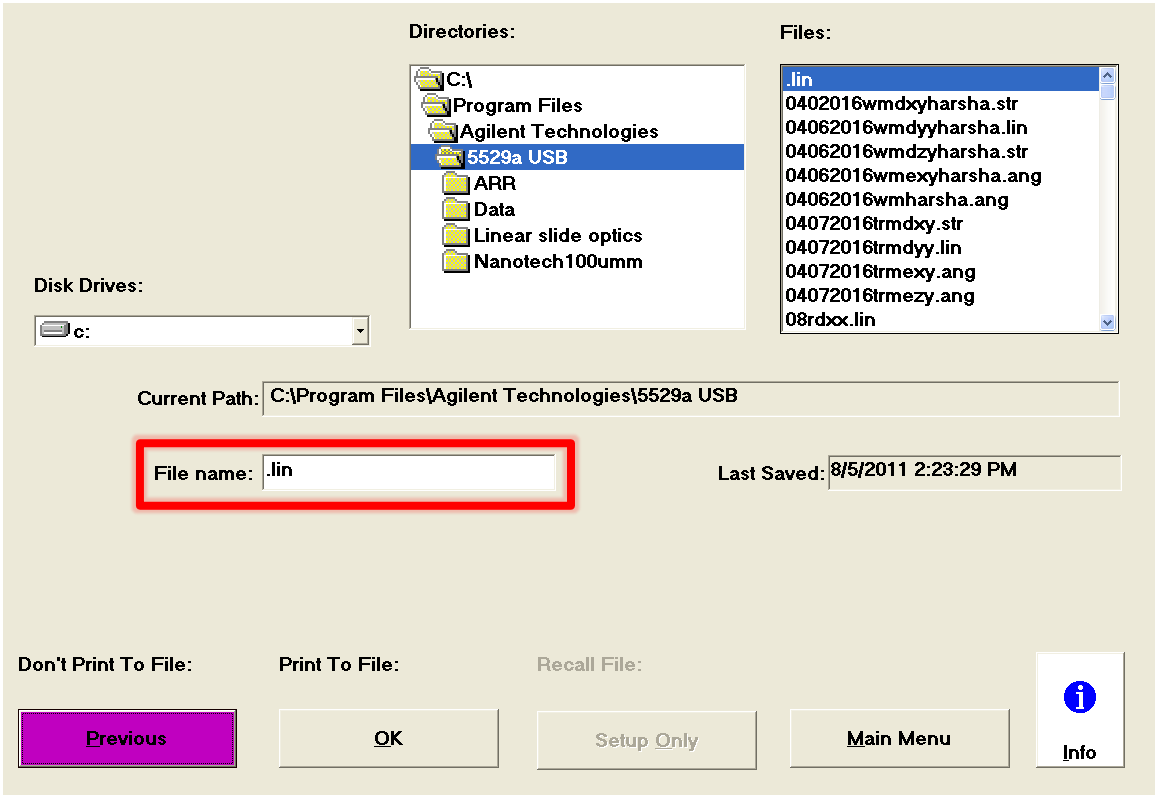

Figure 45: Step 9

Electromagnet Control

To properly control the electromagnet a polarity switching circuit needs to be implemented. The purpose of the four relays is to switch the polarity of the magnet followed disconnecting the power. Relays 1 and 2 activate simultaneously to switch the polarity. Relays 3 and 4 activate simultaneously to turn the power on and off.

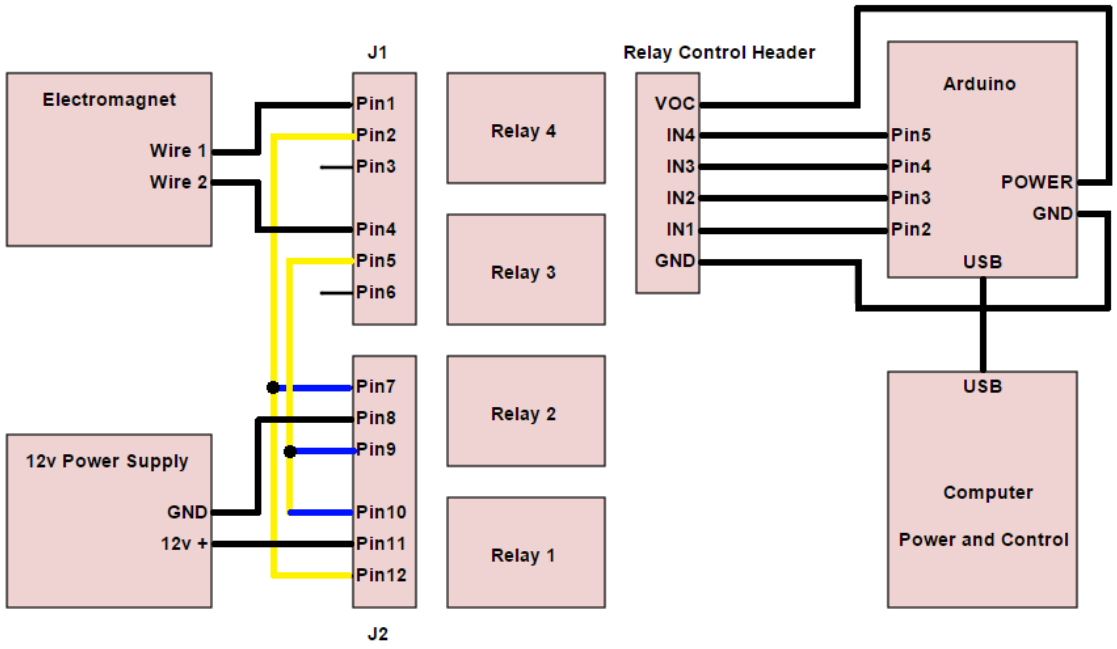

Figure 46: Electromagnet Control Diagram

Selecting Normal Force

Selecting the proper normal force for the mechanism is critical for certain materials. The nominal diameter of the sample is 6.35 mm (0.25”). Table 4 shows the appropriate mass to be added to the top of the shaft for a given pressure.

Table 4: Mass Selection

Pressure (MPa)	Mass (kg)
0.2	0.405
0.4	1.051
0.6	1.697
0.8	2.342
1.0	2.988
1.2	3.634
1.4	4.279
1.6	4.925
1.8	5.571
2.0	6.216

Alternatively, given the mass of the shaft and hardware being 0.24 kg, the additional mass required to achieve a given pressure can be calculated using:

$$M = P \cdot 3.228 - 0.24$$

where:

$M = mass\ (kg)$

$P = Pressure\ (MPa)$

Friction Sample Template

Friction measurement requires two material samples to be cut to size and mounted to the FMM machine. One sample is attached to the hardened steel shaft, while the other sample is bolted to the moving platform as depicted in Figure 47.

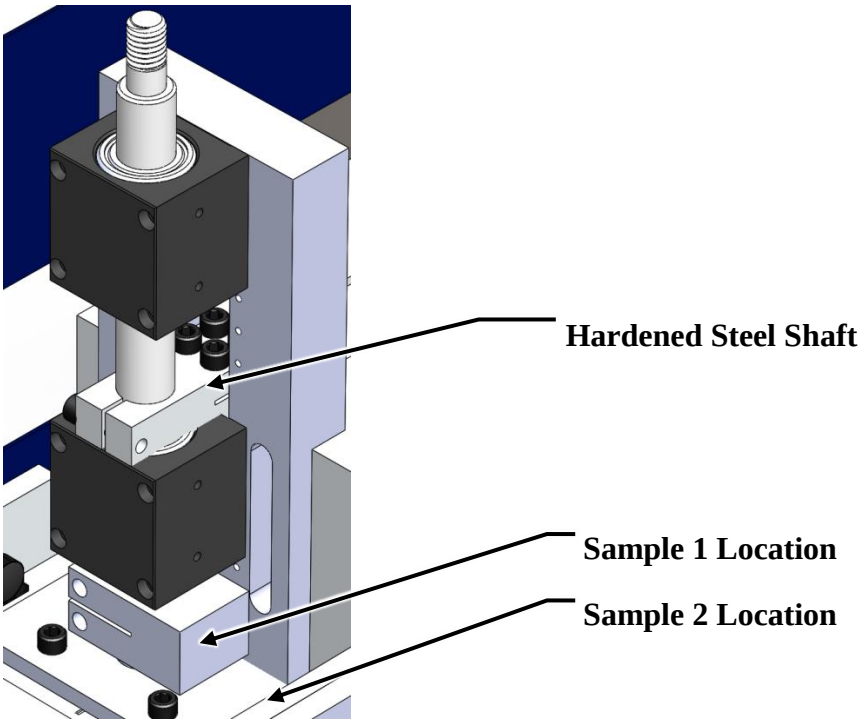

Figure 47: Sample Setup

Sample 1 Dimensions

The sample that is attached to the hardened steel shaft, sample 1, should be dimensioned as shown in Figure 48. The diameter of the sample should be selected, such that it forms a temporary press fit with a 6.35 mm (0.25”) counter-bored hole in hardened steel.

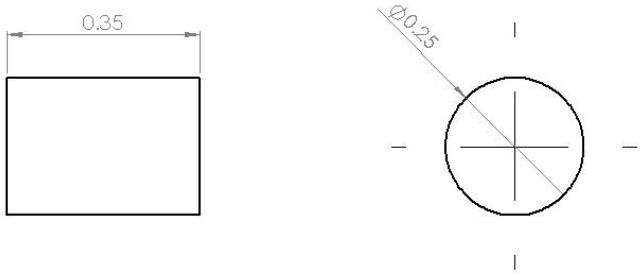

Figure 48: Sample 1 Dimensions (inches)

Sample 2 Dimensions

The sample mounted to the moving platform of the FMM should be prepared with two holes located 50.8 mm (2”) apart. The FMM contains several ¼-20 holes in a 25.4 mm (1”) grid for mounting the sample. The size of the sample can be altered as long as it maintains the proper hole spacing and mounting locations do not interfere with the mating surfaces.

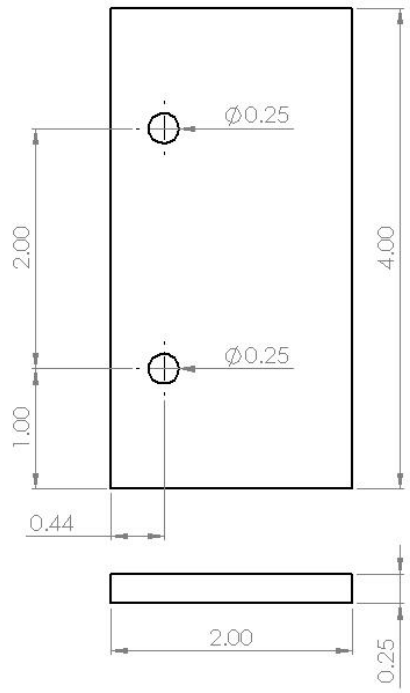

Figure 49: Sample 2 Dimensions (inches)

Figure 23 shows a suitable layout for the preparation of sample 2. The thickness of the sample is not strictly set at 6.35 mm (0.25”). However, it is recommended that sample 2 is nominally 6.35 mm (0.25”) thick so that the friction force caused by the two mating surfaces as they slide relative to each other is on the centerline of the flexure. This reduces any moments places the contact along the same line as the displacement measuring interferometer.

Sample Preparation

Sample preparation is important because, depending on the surface finish and the contacting area of the samples, the friction behavior may differ. The surface finish of the samples should be prepared in the same manner as the surface finish of the application. In other words, if the goal is to measure the coefficient of friction between a polished stainless steel surface and a rough polycarbonate surface, these samples should be prepared in that fashion. After the two samples have been inserted into their respective locations, sample 1's surface should be parallel to sample 2's surface. To insure the parallelism of the two samples, sandpaper or other abrasive material is inserted between the two surfaces as shown in Figure 50.

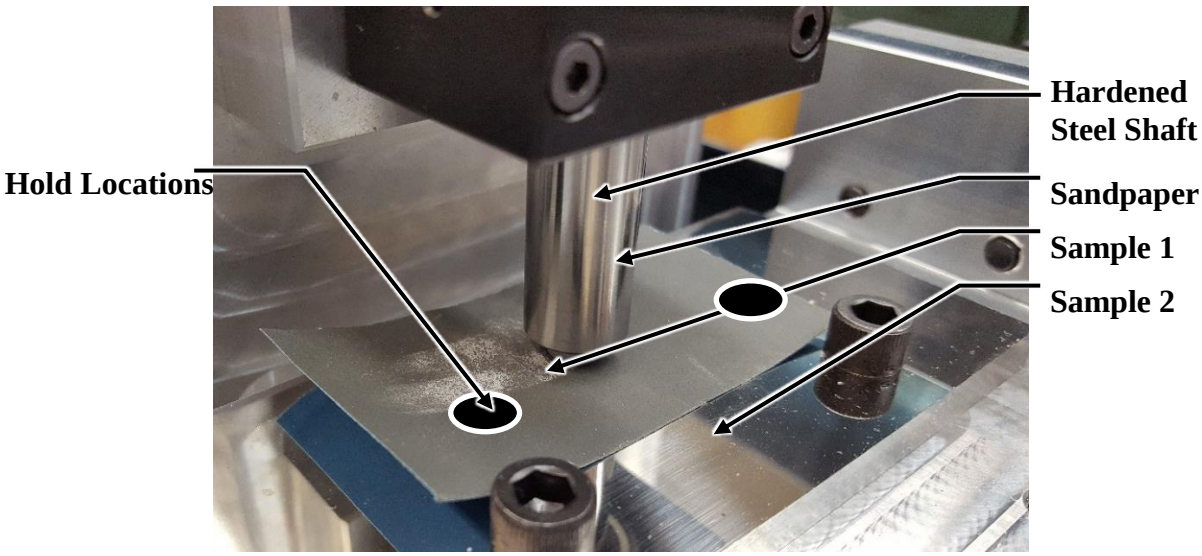

Figure 50: Preparing Sample for Test

After the sandpaper is inserted between the two samples hold it in place on the left and right side as indicated by the hold locations in Figure 50. While holding the sandpaper, manually actuate the flexure until the entire surface is contacting the sandpaper. Next use a few increasing grit sandpapers to obtain the proper surface finish.